macromol

MDPI

Review

Recent Advances on Glyoxylates and Related Structures as Photoinitiators of Polymerization

Frédéric Dumur

Aix Marseille Univ, CNRS, ICR, UMR 7273, F-13397 Marseille, France; frederic.dumur@univ-amu.fr

Abstract: The design of photoinitiators activable under low-light intensity is an active research field, supported by the recent energetic sobriety plans imposed by numerous countries in Europe. With an aim to simplify the composition of the photocurable resins, Type I photoinitiators are actively researched as these structures can act as monocomponent systems. In this field, a family of structures has been under-investigated at present, namely, glyoxylates. Besides, the different works carried out in three years have evidenced that glyoxylates and related structures can be versatile for the design of Type I photoinitiators. In this review, an overview of the different glyoxylates and related structures reported to date is provided.

Keywords: glyoxylate; methyl benzoyl formate; water-soluble; Type I photoinitiators; low-light intensity; LEDs

Citation: Dumur, F. Recent Advances on Glyoxylates and Related Structures as Photoinitiators of Polymerization. *Macromol* **2023**, *3*, 149–174. https://doi.org/10.3390/macromol3020010

Academic Editor: Ana María Díez-Pascual

Received: 27 March 2023
Revised: 18 April 2023
Accepted: 19 April 2023
Published: 23 April 2023

1. Introduction

During the past decade, photopolymerization has witnessed intense research efforts, supported by the development of more and more applications making use of photopolymerization, but also by the gradual abandonment of conventional UV curing using mercury lamps in favor of more energy-efficient LED-triggered polymerization processes [1]. Notably, the recent development of light-emitting diodes (LEDs) that are cheap, compact, lightweight, and energy-saving devices has discarded the historical UV irradiation setups that are expensive and energy-consuming devices [2–9]. Parallel to this, UV photopolymerization is facing numerous criticisms such as safety concerns (eye and skin damage) or the production of ozone during photopolymerization [10,11]. Intense efforts existing at present to develop photoinitiating systems absorbing visible light are also supported by the different applications using photopolymerization and 3D and 4D printing, dentistry, adhesives, solvent-free paints, microelectronics, coatings and varnishes can be cited as relevant examples [12–25].

Another point of interest concerns one of the most components of photocurable resins, namely the chromophore that interacts with light and can generate radicals in the presence of co-initiators and additives [10,11,26,27]. Indeed, photoinitiators can be divided into two different categories. The first one concerns Type II photoinitiators. In this case, photoinitiators are not capable to initiate a polymerization alone and additives have to be used. Notably, Type II photoinitiators are commonly combined with hydrogen/electron donors so that after a photoinduced electron transfer followed by a hydrogen abstraction reaction, initiating species can be generated. Parallel to this first mechanism, Type II photoinitiators can also be combined with onium salts (sulfonium or iodonium salts) so that aryl radicals can be formed after a photoinduced electron transfer. To render the system catalytic, a sacrificial amine can be used, enabling to introduction of the photosensitizer in a catalytic amount. Parallel to this first category, Type I photoinitiators can act as monocomponent systems, greatly simplifying the composition of the photocurable resins. The generation of initiating radicals is based on the homolytic cleavage of a selected bond (See Scheme 1). As the main drawback of this approach, the photodecomposition of Type I photoinitiators

results in the irreversible consumption of the molecule, so that the concentration of radicals drastically decreases over time. However, concerning this last point, the irreversible consumption of photoinitiators is also true for Type II photoinitiators when two-component photoinitiating systems. This is notably the case for the amines/thioxanthone photoinitiating systems where the thioxanthone is consumed during the electron/proton transfer initiating step [28,29]. Among Type I photoinitiators that have been extensively studied, hexaaryl biimidazoles (HABIs), phosphine oxides, oxime esters, benzoin derivatives, benzylketals, acyloximino esters, trichloromethyl-*S*-triazines, *o*-acyl-α-oximino ketones, α-aminoalkylacetophenones, or hydroxyacetophenones can be cited as the most common structures [30–32].

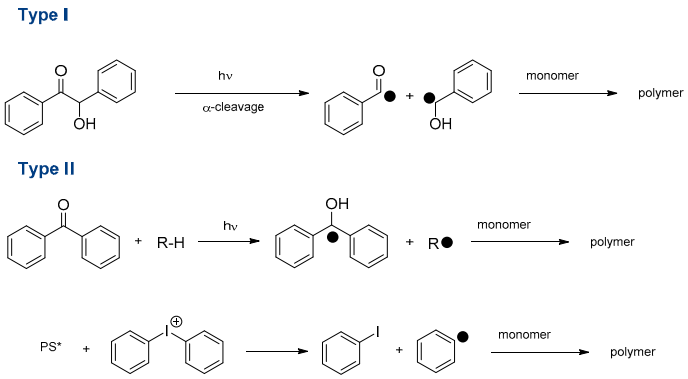

Scheme 1. Radical generation with Type I and Type II photoinitiators. (* corresponds to the excited state of PS).

The reactivity of photoinitiators and the light penetration that can be achieved within the photocurable resin is also strongly related to the wavelength used for photoinitiation. Indeed, as shown in Figure 1, light penetration can vary from a few hundreds of micrometers up to a few centimeters, depending on the fact that photopolymerization is mostly carried out in the wavelength range between 350 nm and 800 nm [33]. By polymerizing at longer wavelengths, a higher light penetration can be obtained within the photocurable resin. Access to filled samples is also possible [34].

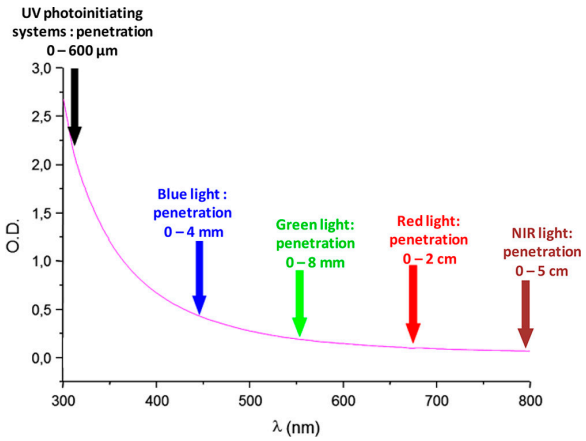

Figure 1. Light penetration in polystyrene latex with an average diameter of 112 nm. Reprinted with permission from Ref. [33], Copyright 2018, The American Chemical Society.

However, by polymerizing at long wavelengths, photons are also less energetic than UV photons so this issue can only be addressed by developing photoinitiating systems facilely producing initiating species in unfavorable low energetic conditions. This is the reason why after approximately two decades, a wide range of structures have

been examined, as exemplified by benzophenones [35–42], thioxanthones [43–58], camphorquinones [59,60], curcumin [61–64], chromones and flavones [65–67], acridine-1,8-diones [68–70], pyrenes [71–79], anthracenes [80], carbazoles [81–96], benzylidene ketones [97–104], cyclohexanones [105–108], chalcones [20,109–124], cyanines [125–131], push-pull dyes [3,4,132–146], bodipy [43,147–151], coumarins [152–165], naphthalimides [166–184], iodonium salts [43,166,185–193], perylenes [194–197], diketopyrrolopyrroles [198], and quinoxalines [199–212], to cite a few. However, in the aforementioned list, if only purely organic dyes have been cited, metal complexes (iridium [213,214], ruthenium [215], copper [216–218], iron [219], zinc [220]) or purely inorganic structures (perovskites [221], metal–organic frameworks [222], metal particles [223], quantum dots [224]) can also be cited as photoinitiators of polymerization. By investigating these different structures, water-soluble [225], photobleachable [226] photoinitiators, or photoinitiators activable with sunlight [7,227,228] have been identified. Besides, during the last five years, a significant effort has been devoted to developing Type I photoinitiators greatly simplifying the composition of the photocurable resins. Indeed, efficient multicomponent photoinitiating systems are difficult to prepare and the lack of stability by undesired reactions between the different additives constitutes the major drawback of this approach. With the aim of developing Type I photoinitiators, a family of photocleavable dyes has only been scarcely investigated in the literature, namely glyoxylates. These structures that are also sometimes named keto esters can easily cleave between the two carbonyl groups, producing initiating radicals. If methyl benzoylformate (MBF) is a commercially available UV photoinitiator, this scaffold has not been a source of inspiration for photopolymerists for the design of new photoinitiators and only a few derivatives of this structure have been reported in the literature.

In this review, an overview of the different glyoxylates and related structures reported to date is provided. This family of dyes is of crucial interest for the future development of photoinitiators of photopolymerization.

2. Glyoxylates and Related Structures

2.1. Glyoxylate Derivatives

In 2021, a series of glyoxylate derivatives have been proposed by Sun and coworkers, bearing electron-donating or electron-accepting groups (See Figure 2) [229]. By means of this specific substitution, photopolymerization experiments could be carried out at 405 nm. In this series of dyes, dimethyl 1,4-dibenzoylformate (DM-BD-F) proved to be the most efficient photoinitiator during the free radical polymerization (FRP) of acrylates (tri (propylene glycol)diacrylate (TPGDA) or trimethylolpropane triacrylate (TMPTA)), resulting from its unique ability to produce twice more radicals than the nine other structures. To determine the real performance of the different glyoxylate derivatives, phenylbis (2,4,6-trimethylbenzoyl)phosphine oxide (BAPO), and dibenzoyl (DB) were used as reference photoinitiators.

Due to the weak absorption of the different dyes at 405 nm, deep layer photocuring could also be obtained and a polymer thickness of 6.5 cm could be polymerized within 30 s. Parallel to this, due to the weak absorption of glyoxylate derivatives at 385, 395, and 405 nm, almost colorless coatings could be produced. From the absorption viewpoint, major differences could be found between the different dyes in acetonitrile (See Table 1 and Figure 3).

Interestingly, compared to the parent methyl benzoyl formate (MBF), all derivatives exhibited a redshifted absorption, except for TF-MBF exhibiting the strong electron-withdrawing group. Logically, the most redshifted absorptions were found for all dyes comprising an electron-donating group inducing an efficient intramolecular charge transfer (ICT) through a push-pull effect. Thus, N-MBF and S-MBF both exhibited the most redshifted absorptions located at 356 and 326 nm respectively, together with the highest molar extinction coefficients (43,800 $M^{-1} \cdot cm^{-1}$ and 29,660 $M^{-1} \cdot cm^{-1}$ respectively). Compared to BAPO, N-MBF exhibited higher molar extinction coefficients at all wavelengths later used for photopolymerization. Photolysis experiments revealed the occurrence of a de-

carboxylation reaction using bromocresol green as the pH indicator. Consistent with the mechanism established in the literature, a decarboxylation reaction occurring subsequent to the photocleavage was proposed, as shown in Scheme 2.

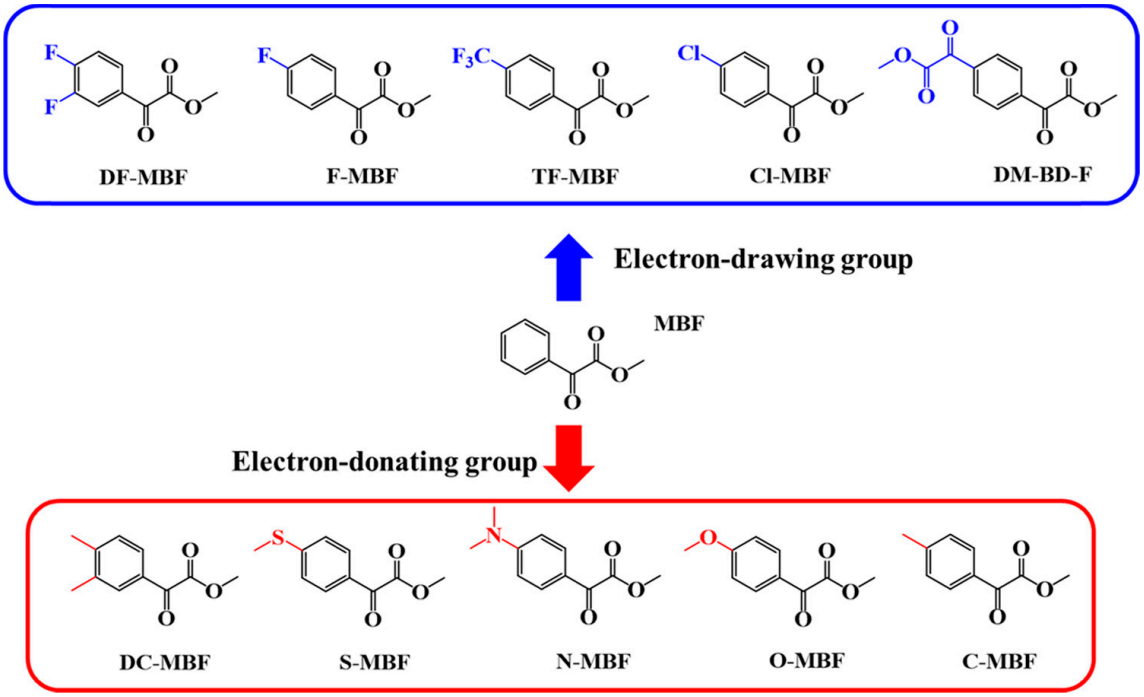

Figure 2. Chemical structures of different glyoxylate derivatives exhibiting electron-donating and electron-accepting groups. Reproduced with the permission of Ref. [229]. Copyright 2021. The American Chemical Society.

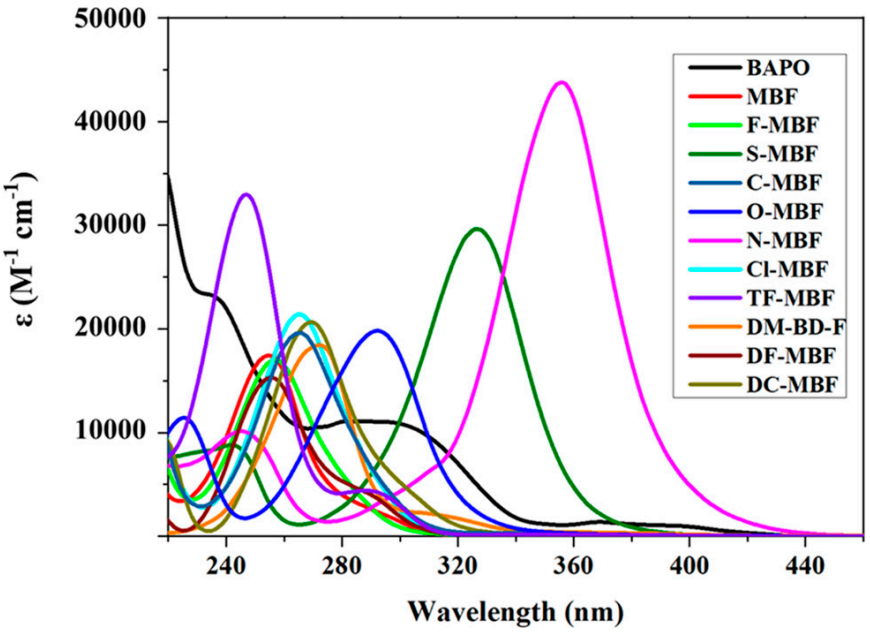

Figure 3. UV-visible absorption spectra of different glyoxylates derivatives recorded in acetonitrile. Reproduced with permission of Ref. [229]. Copyright 2021. The American Chemical Society.

Table 1. Molar extinction coefficients ($M^{-1} \cdot cm^{-1}$) of the different glyoxylate derivatives in acetonitrile, at the maximum absorption and different wavelengths used for photopolymerization.

Photoinitiator	λ_{max} (nm)	εmax	ε385	ε395	ε405	ε455
BAPO	-	-	1100	1020	770	0
MBF	255	17,430	30	10	10	0
F-MBF	257	16,760	30	20	10	0
S-MBF	326	29,660	590	260	110	0
C-MBF	266	19,630	60	40	30	10
O-MBF	290	19,830	120	90	70	40
N-MBF	356	43,800	12,180	6660	3600	80
Cl-MBF	265	21,420	60	40	30	0
TF-MBF	246	32,800	110	80	50	10
DM-BD-F	273	18,440	280	220	160	50
DF-MBF	256	25,350	110	90	70	20
DC-MBF	269	20,690	100	40	30	10

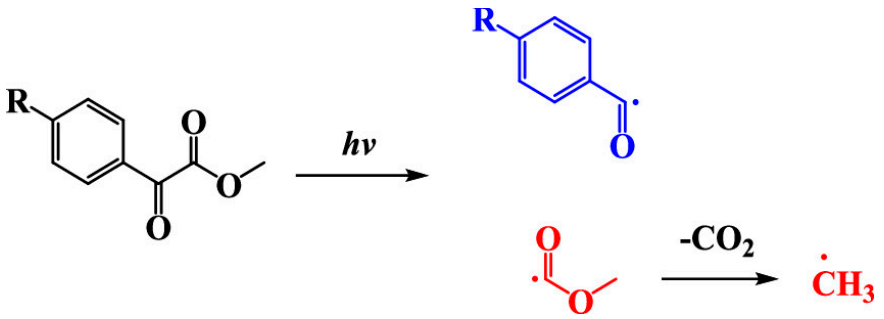

Scheme 2. Mechanism of radical generation with glyoxylates. Reproduced with permission of Ref. [229]. Copyright 2021. The American Chemical Society.

By theoretical calculations, the bond dissociation energy (BDE) of the different derivatives could be determined, and values ranging between 108.40 kJ/mol for TF-MBF and 150.94 kJ/mol for N-MBF were calculated (See Table 2). Parallel to this, the ΔH of all MBFs was determined as being negative, meaning that the cleavage reaction was energetically favorable [230].

Table 2. Bond dissociation energies (kJ/mol) were determined for different glyoxylates.

Photoinitiator	BDE
MBF	138.98
F-MBF	137.92
S-MBF	148.85
C-MBF	138.30
O-MBF	145.18
N-MBF	150.94
Cl-MBF	140.55
TF-MBF	108.40
DM-BD-F	118.83
DF-MBF	134.76
DC-MBF	140.28

Examination of their photoinitiating abilities during the FRP of TPGDA revealed F-MBF to furnish a higher monomer conversion than BAPO (See Figure 4 and Table 3). Excellent monomer conversions could also be obtained with the other MBFs, except S-MBF and O-MBF for which conversions lower than 40% could be determined. The low reactivity of these derivatives was confirmed during the FRP of TMPTA. However, contrary to what was observed in TPGDA, none of the MBFs could outperform BAPO. Thus, if a TMPTA conversion of 59.4% could be obtained with BAPO, the best conversion with MBFs was obtained with O-MBF, peaking at 49.6%. The lower monomer conversion obtained with TMPTA compared to TPGDA was assigned to the higher viscosity of TMPTA and its trifunctionality.

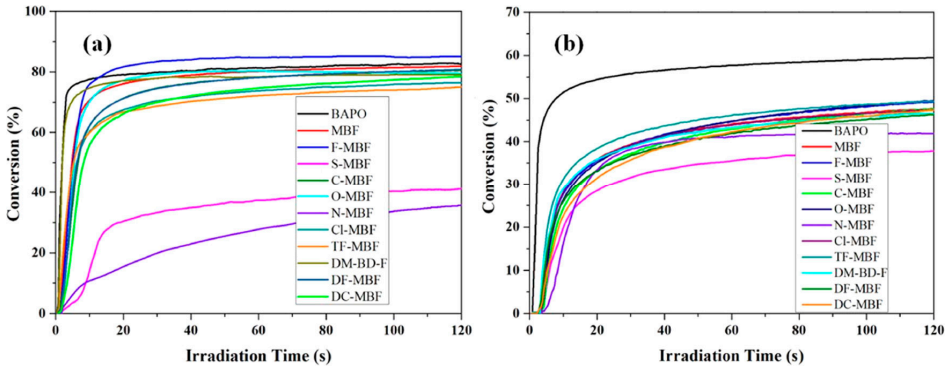

Figure 4. Photopolymerization profiles of (**a**) TPGDA and (**b**) TMPTA in laminate using the different MBFs or BAPO (1 wt%) upon irradiation at 405 nm. Reproduced with permission of Ref. [229]. Copyright 2021. The American Chemical Society.

Table 3. TPGDA and TMPTA conversions after 120 s upon irradiation at 405 nm.

Photoinitiator	TPGDA	TMPTA
BAPO	82.8	59.4
MBF	81.6	47.7
F-MBF	85.1	49.3
S-MBF	41.6	38.2
C-MBF	80.4	47.7
O-MBF	79.4	49.6
N-MBF	36.5	42.0
Cl-MBF	76.5	47.3
TF-MBF	75.6	49.3
DM-BD-F	79.1	46.8
DF-MBF	80.7	46.2
DC-MBF	78.3	47.7

Noticeably, DM-BD-F could maintain an excellent monomer conversion with the two monomers, resulting from its unique ability to produce double radicals compared to the other MBFs. Overall, the following trend could be established: if the presence of electron-accepting groups could improve the monomer conversion, the opposite situation was found for the electron-donating groups. Indeed, in this series of dyes, N-MBF and S-MBF exhibiting the highest molar extinction coefficients also demonstrated the lowest photoinitiating abilities, evidencing that absorption was not the only parameter governing the photoreactivity. Determination of the enthalpy of the reaction revealed ΔH to be negative for all MBFs. Besides, if the cleavage reaction was determined as being energetically favorable, the photoinitiating capability is also strongly related to the values of ΔH. Thus, if DM-BD-F and TF-MBF exhibited ΔH values of -127.89 and -111.46 kJ/mol respectively,

these values were only reduced to −68.87 and −72.57 kJ/mol for S-MBF and N-MBF respectively, explaining their lower photoinitiating abilities.

Finally, examination of the depth of cure for TPGDA after 30 s of irradiation at 405 nm with the different systems revealed F-MBF TF-MBF, and DM-BD-F to furnish a curing depth of 5.0, 6.3, and 6.5 cm respectively, greatly higher than that of BAPO (1.0 cm) (See Figure 5). Noticeably, good photobleaching could be obtained during photopolymerization so that colorless polymers could be obtained with all MBFs.

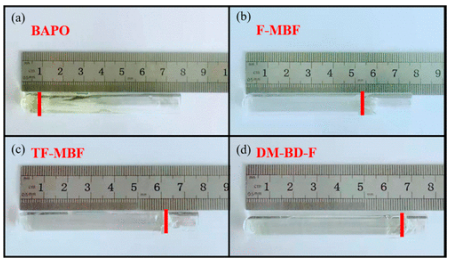

Figure 5. Depth of cure determined in TPGDA upon irradiation at 405 nm for 30 s. Reproduced with permission of Ref. [229]. Copyright 2021. The American Chemical Society.

2.2. Cinnamoyl Formate Derivatives

In 2022, the same group examined a new family of dyes derived from methyl benzoylformate (MBF), namely ethyl cinnamoyl formates (ECFs) [231]. Four structures were investigated, two of them bearing an electron-donating group (S-ECF and O-ECF) and one structure with an electron-accepting group (F-ECF) (See Scheme 3). The different dyes could be prepared by a two-step synthesis consisting first of a Claisen Schmidt condensation followed in the second step by an esterification reaction. F-ECF, S-ECF, and O-ECF could be prepared with reaction yields of 60, 55, and 59% for the two steps respectively.

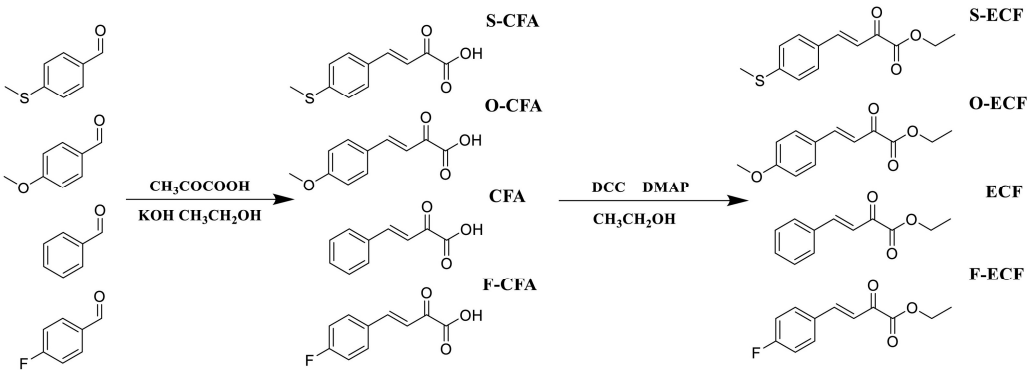

Scheme 3. Chemical structures of the different ECFs. Reproduced with permission of Ref. [231]. Copyright 2022, Elsevier.

Examination of their absorption properties in acetonitrile revealed the shift of the absorptions to be comparable to that observed for the previous MBFs. Thus, the introduction of electron-donating groups redshifted the absorption (S-ECF and O-ECF) whereas the opposite effect was found in the presence of electron-accepting groups (F-ECF) (See Figure 6 and Table 4). The most redshifted absorption was found for S-ECF, peaking at 362 nm. Irrespective of the substitution pattern, almost similar molar extinction coefficients could be found for the different dyes.

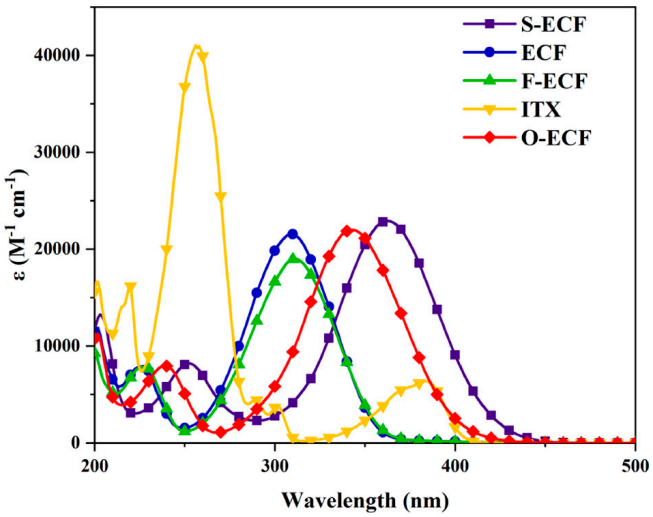

Figure 6. UV-visible absorption spectra of the different ECFs in acetonitrile. Reproduced with the permission of Ref. [231]. Copyright 2022, Elsevier.

Table 4. Molar extinction coefficients of ECFs in acetonitrile at the maximum absorption, 405 nm, and 455 nm.

Photoinitiator	λ_{max} (nm)	ε_{max} ($M^{-1}\cdot cm^{-1}$)	ε_{405nm} ($M^{-1}\cdot cm^{-1}$)	ε_{455nm} ($M^{-1}\cdot cm^{-1}$)
ECF	309	21,550	130	0
F-ECF	309	18,890	130	0
O-ECF	342	22,000	1730	10
S-ECF	362	22,930	7060	80
ITX	256	41,050	610	0

Photolysis experiments carried out in acetonitrile revealed the different ECFs to be unable to generate radicals alone. Upon addition of ethyl dimethylaminobenzoate (EDB), a fast photolysis process could be evidenced and the formation of α-aminoalkyl radicals was confirmed by electron spin resonance (EPR) experiments. Overall, the mechanism of radical generation proposed in Scheme 4 was suggested. The initiation mechanism is that of a type II photoinitiator. Thus, upon photoexcitation, a photoinduced electron transfer between EDB and ECFs can occur, generating EDB radical cations and ECF radical anions. In the second step, a hydrogen abstraction reaction can occur, generating α-aminoalkyl radicals on EDB and constituting the initiating species. It has to be noticed that the different radicals formed during photolysis have been identified by electron spin resonance (ESR) experiments.

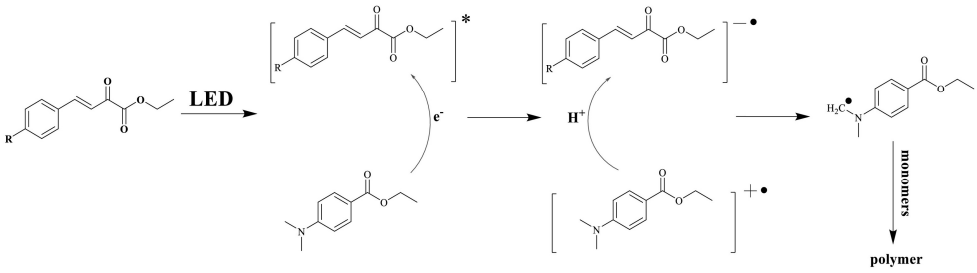

Scheme 4. Initiation mechanism evidenced for all ECFs. Reproduced with the permission of Ref. [231]. Copyright 2022, Elsevier.

Polymerization tests carried out at 405 nm and 455 nm during the FRP of TPGDA revealed O-ECF to outperform the reference photoinitiator 2-isopropylthioxanthone (ITX) during the 20 first seconds of irradiation (See Figure 7 and Table 5). After 240 s of irradiation, all ECFs could furnish monomer conversions comparable to that of ITX at 405 nm. Noticeably, no significant difference in monomer conversions could be observed between ECFs substituted with electron-donating or electron-accepting groups. At 455 nm, a higher variation of the monomer conversion was found, attributable to differences in absorption at this specific wavelength.

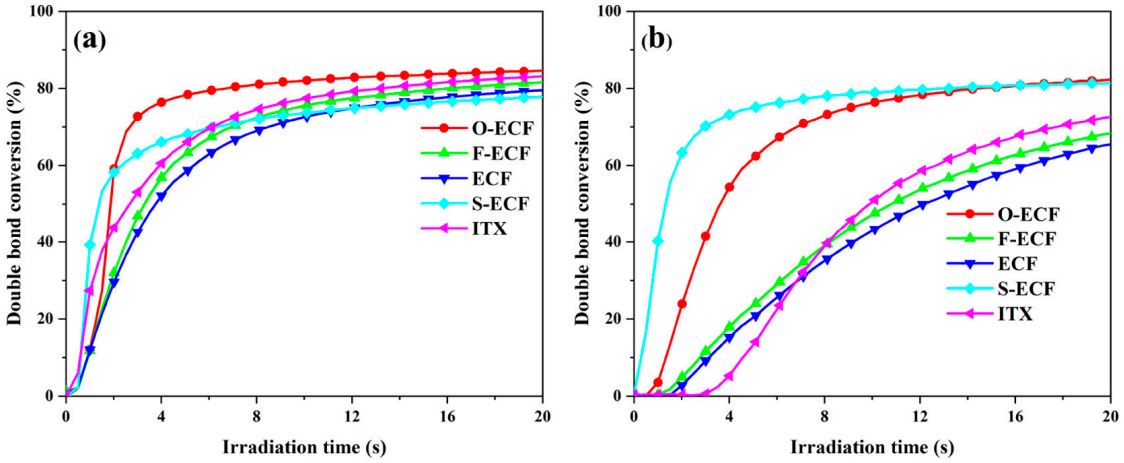

Figure 7. TPGDA conversions were obtained upon irradiation at 405 nm (**a**) and 455 nm (**b**) for 240 s. Reproduced with the permission of Ref. [231]. Copyright 2022, Elsevier.

Table 5. TPGDA conversions after 240 s upon irradiation at 405 and 455 nm.

Photoinitiators	ITX	O-ECF	S-ECF	F-ECF	ECF
Conversion at 405 nm	92.3	91.1	86.9	89.9	88.5
Conversion at 455 nm	91.8	89.3	87.2	88.4	89.7

Here again, a good photobleaching of the resins could be evidenced, especially with S-ECF which is the dye exhibiting the most redshifted absorption of the series (See Figure 8). This result is remarkable considering that an opposite situation was found for ITX. Indeed, as shown in Figure 8, yellowing of the sample could be demonstrated after polymerization, despites the lack of color for the initial solution. By nuclear magnetic resonance (NMR), the authors demonstrated the photobleaching to originate from the suppression of the π-conjugated system, with the disappearance of the central double bond, therefore suppressing the electronic delocalization. Notably, the addition of EDB radicals on the central double bond was confirmed by mass spectrometry.

Considering the excellent photobleaching, the authors also investigated deep-layer polymerization. Using the two-component S-ECF/EDB system, a depth of cure of 7 cm could be determined upon irradiation at 455 nm for 20 min. A low extractability of 0.086% of S-ECF was determined, lower than that of ITX (0.97%). The low extractability of S-ECF is directly related to the photobleaching mechanism, demonstrating that EDB radicals could add on the cinnamoyl system, enabling covalently linking the photoinitiator to the polymer network. However, it could be as well any radicals on the growing polymer chain that can add to the cinnamoyl system, enabling covalently linking the photoinitiator to the polymer network. Low cytotoxicity was also determined for S-ECF. Notably, a cell viability of 98% could be determined for the samples prepared with 20 μg/mL of S-ECF. By increasing the photoinitiator content up to 20 μg/mL, the cell viability was only reduced to 90%, evidencing the good cytocompatibility of S-ECF.

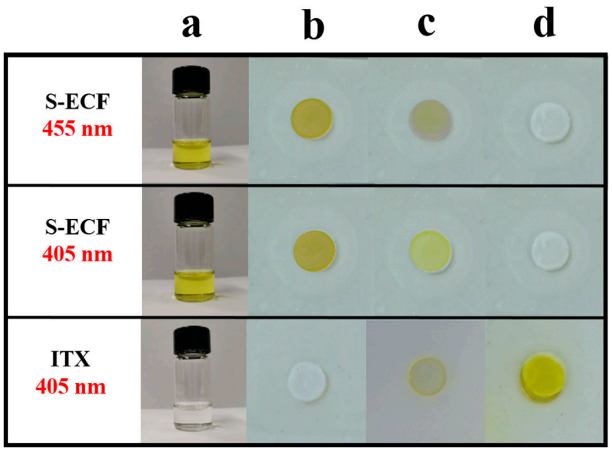

Figure 8. Photobleaching experiments were carried out with the two-component S-ECF/EDB combination. (**a**) initial solution (**b**) sample before irradiation (**c**) after 8 s (**d**) after 15 s of irradiation. Reproduced with the permission of Ref. [207]. Copyright 2007, Elsevier.

2.3. Silyl Glyoxylates

In 2017, Lalevée and coworkers proposed a new family of glyoxylate, namely silyl glyoxylates (See Figure 9) [232,233]. *Tert*-butyl (*tert*-butyldimethylsilyl)glyoxylate (DKSi), ethyl(*tert*-butyldimethyl)silyl glyoxylate (Et-DKSi), and benzyl (*tert*-butyldimethyl)silyl glyoxylate (Bn-DKSi) were examined as monocomponent photoinitiating systems or in combination with additives (See Figure 10) for the FRP of a dental resin, namely a Bis-GMA/TEGDMA (70/30 *w*/*w*) blend (where BisGMA and TEGDMA stand for bisphenol A-glycidyl methacrylate and triethylene glycol dimethacrylate respectively) or urethane dimethacrylate (UDMA).

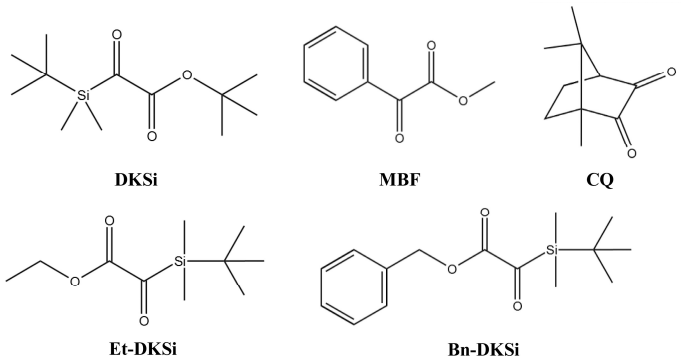

Figure 9. Chemical structures of different silyl glyoxylates investigated by Lalevée and coworkers. Reproduced with the permission of Ref. [232]. Copyright 2007, Elsevier.

Examination of the absorption properties of DKSi in toluene revealed the absorption maximum to be located at 425 nm, therefore blueshifted compared to that of camphorquinone (CQ) (465 nm). Besides, compared to the previous MBF, a significant enhancement of the molar extinction coefficient could be evidenced at 405 nm (See Figure 11). By theoretical calculations, the redshift of the absorption maximum was determined as originating from a strong participation of the d orbital of the Si atom to the highest occupied molecular orbital (HOMO) and the lowest unoccupied molecular orbital (LUMO), decreasing the HOMO-LUMO gap compared to that of the previous MBF (4.19 eV for DKSi vs 4.71 eV for MBF). A good overlap between the emission of the LED emitting at 477 nm and DKSi and camphorquinone was thus found.

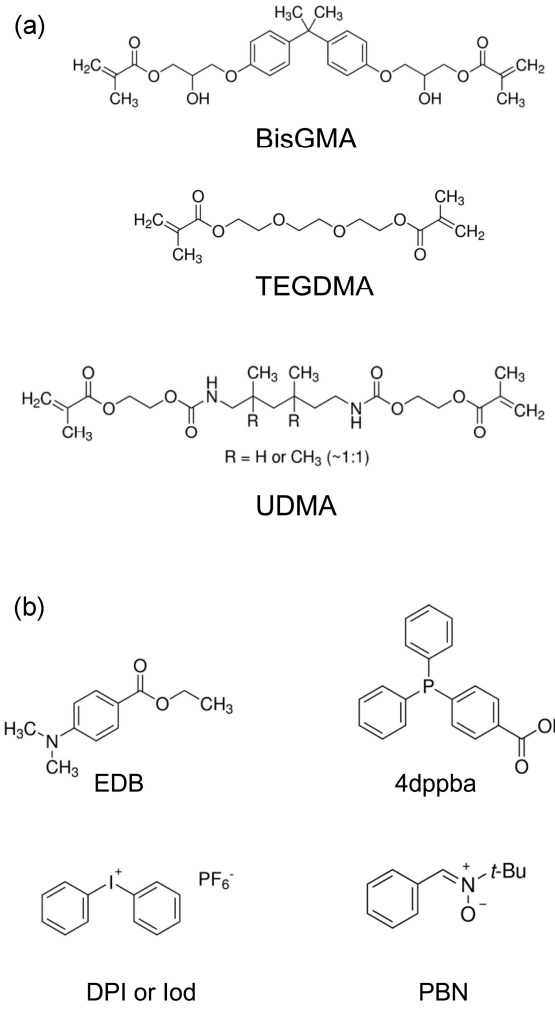

Figure 10. Chemical structures of the different monomers and additives used with silyl glyoxylates. Reproduced with permission of Ref. [232].

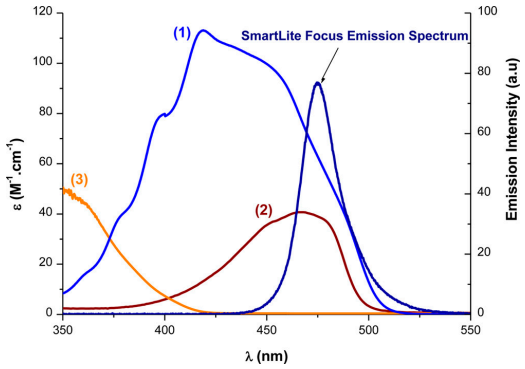

Figure 11. UV-visible absorption spectra of (1) DKSi in toluene, (2) CQ, and (3) MBF in acetonitrile. Reproduced with permission of Ref. [232]. Copyright 2017. The American Chemical Society.

During the FRP of the BisGMA/TEGDMA blend, the ability of DKSi to act as a monocomponent system was demonstrated in laminate. After 80 s of irradiation, a conversion of 40% could be determined. Upon the addition of EDB, the conversion drastically increased and a conversion of 68% was obtained. Under air and due to strong oxygen inhibition in thin films, DKSi alone was almost unable to initiate the FRP of the resin. Conversely, the three-component DKSi/EDB/DPI (2/1.4/1.6% *w*/*w*/*w*) system could furnish

a monomer conversion of 33%, which could be improved by using the four-component DKSi/EDB/DPI/CQ (2/1.4/1.6/1% *w*/*w*/*w*/*w*) system (38%) (See Figure 12). Improvement of the monomer conversion obtained with the four-component system compared to the three-component system can be assigned to improved light absorption properties due to the concomitant presence of DKSi and CQ, both contributing to light absorption.

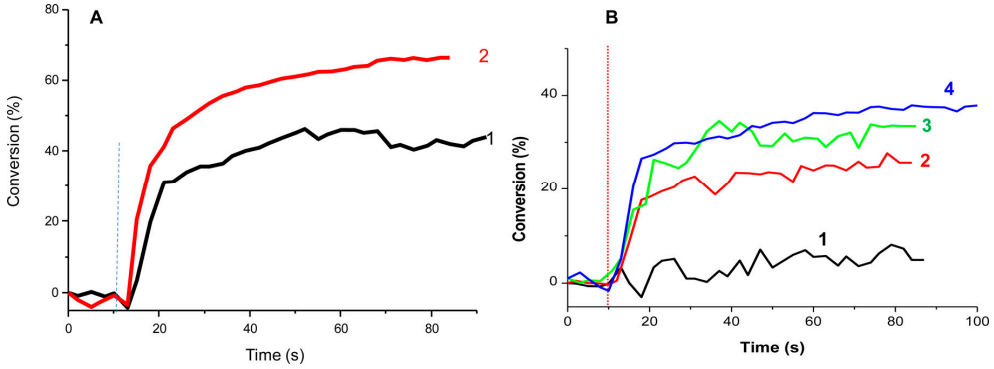

Figure 12. Polymerization profiles determined for a BisGMA/TEGDMA blend upon irradiation at 477 nm (I = 300 mW/cm^2) in thin films using (**A**) In laminate: (1) DKSi (5wt%); (2) DKSi/EDB (5%/2% *w*/*w*). (**B**) Under air: (1) DKSi (2wt%); (2) DKSi/EDB (2/1.4% *w*/*w*); (3) DKSi/EDB/DPI (2/1.4/1.6% *w*/*w*/*w*); (4) DKSi/EDB/DPI/CQ (2/1.4/1.6/1% *w*/*w*/*w*/*w*). Reproduced with permission of Ref. [232]. Copyright 2017. The American Chemical Society.

Investigation of the FRP of UDMA revealed the monomer conversion to increase with the photoinitiator content. Besides, by varying the content from 0.5 to 5 wt%, an optimum concentration at 2 wt% could be determined (See Figure 13).

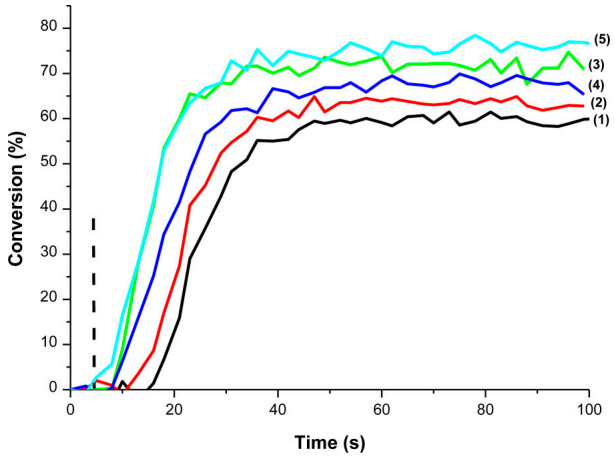

Figure 13. Polymerization profiles of 1.4 mm thick samples of UDMA resin upon irradiation at 477 nm (I = 80 mW/cm^2) under air using DKSi (1) 0.5 wt%, (2) 1wt%, (3) 2 wt%, (4) 3 wt%, (5) 5 wt%. Reproduced with permission of Ref. [232]. Copyright 2017. The American Chemical Society.

For dental applications, photobleaching is an important property. Good bleaching ability could be demonstrated with the two-component DKSi/EDB combination (see Figure 14). Interestingly, after nine months of storage, no modification of the color of the polymer film was detected for the samples prepared with the DKSI/EDB system. A different situation was found for the reference CQ/EDB combination for which a yellowing of the sample could be observed.

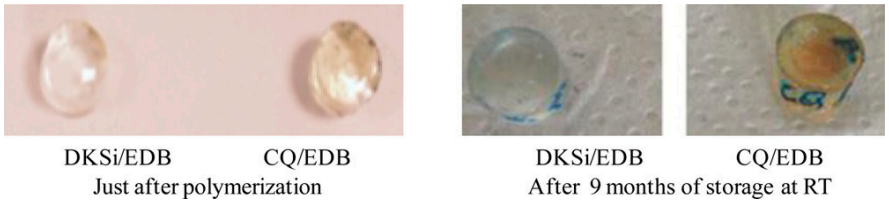

Figure 14. UDMA samples polymerized with different photoinitiating systems (just after irradiation with the LED at 455 nm and after 9 months of storage in the dark); DKSi/EDB (0.5/2% *w*/*w*) and CQ/EDB (0.5/2% *w*/*w*). Reproduced with the permission of Ref. [232]. Copyright 2017. The American Chemical Society.

Excellent monomer conversions could also be obtained using 4-diphenylphosphinobenzoic aid acid as the additive. The choice of this additive was notably motivated by its ability to efficiently overcome oxygen inhibition by converting the non-reactive peroxyl ROO• radicals as initiating species RO• [234]. Investigation of the substituent effects with Et-DKSi and Bn-DKSi revealed the absorption spectra not to be modified except for the molar extinction coefficients (see Figure 15). When tested as monocomponent systems for the FRP of UDMA (1 wt%), the order of monomer conversions perfectly fit with the order of the molar extinction coefficients, evidencing that the reactivity was governed by the molar extinction coefficients and not by the substitution pattern of silyl glyoxylates. By ESR, the formation of radicals in the close vicinity of Si was detected under an inert atmosphere (radical A). A different situation was found under air. No silyl radicals were detected anymore due to the fast reaction with oxygen, producing peroxyl radicals. Formation of *t*-BuOO• was also detected under air, resulting from a decarboxylation reaction of radical B and subsequent reaction with oxygen (See Scheme 5).

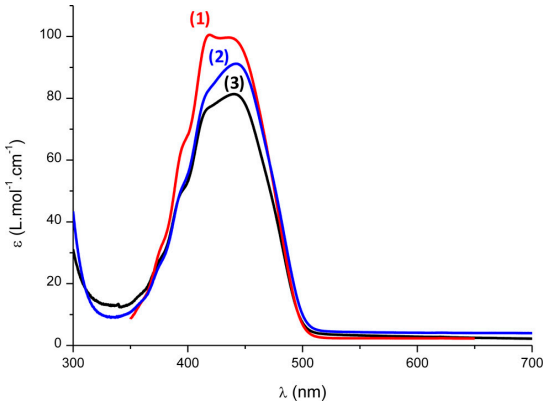

Figure 15. UV-visible absorption spectra of (1) DKSi, (2) Bn-DKSi, and (3) Et-DKSi in acetonitrile. Reproduced with permission of Ref. [232]. Copyright 2017. The American Chemical Society.

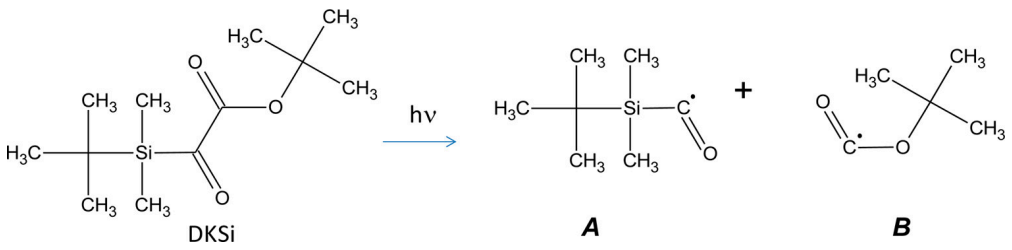

Scheme 5. Radicals formed upon photocleavage of silyl glyoxylates. Reproduced with the permission of Ref. [232]. Copyright 2017. The American Chemical Society.

EPR experiments enabled confirming the chemical structures of the radicals formed upon irradiation (See Scheme 5). In the case of radical B, the occurrence of a decarboxylation reaction was also demonstrated, enabling generating carbon-centered radicals.

2.4. Water-Soluble Benzoylformic Acid Derivatives

The water solubility of photoinitiators is a property that is actively researched with the aim of developing greener polymerization processes [57,96,225,235–239]. Indeed, polymerization in water becomes possible. This point was examined with a series of benzoylformic acid derivatives by the group of Sun and coworkers (See Figure 16) [240].

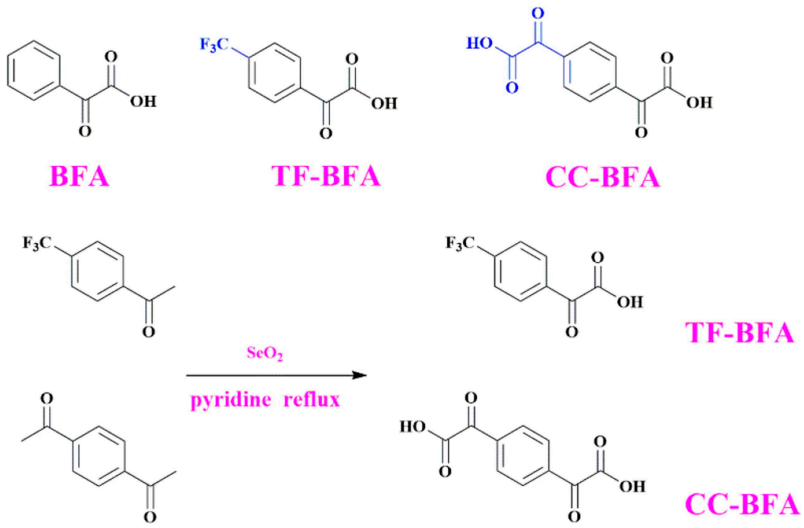

Figure 16. Chemical structures of CC-BFA, TF-BFA, and BFA. Reproduced with permission of Ref. [240]. Copyright 2022. Elsevier.

From the synthetic viewpoint, TF-BFA and CC-TFA could be prepared in one step, by oxidation of the acetyl groups with selenium oxide, and obtained reaction yields of 80 and 62%, respectively. As observed for MBFs and ECFs, the presence of the electron-accepting CF_3 group blueshifted the absorption compared with the parent structure BFA (244 nm for TF-CFA vs. 253 nm for BFA). Conversely, a redshift of the absorption was found for CC-BFA at 262 nm. Interestingly, a significant increase of the molar extinction coefficient was found, peaking at 18,480 $M^{-1}{\cdot}cm^{-1}$ contrarily to 8640 $M^{-1}{\cdot}cm^{-1}$ for BFA and TF-BFA (See Figure 17).

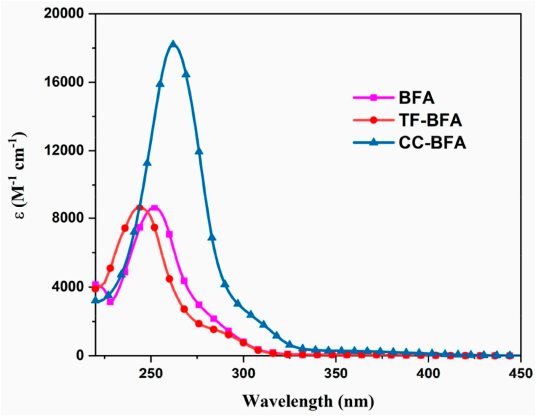

Figure 17. UV-visible absorption spectra of different benzoylformic acids in acetonitrile. Reproduced with permission of Ref. [240]. Copyright 2022. Elsevier.

By theoretical calculations, the BDE of the different dyes could be determined and values of 154.8, 158.6, and 151.9 kJ/mol could be determined for BFA, TF-BFA, and CC-BFA, evidencing that the BDE was only slightly modified by the substitution pattern of benzoylformic acids. Polymerization experiments done at 405 nm for TPGDA and TMPTA revealed CC-TFA to outperform BFA and TF-BFA during the FRP of TPGDA. A conversion of 83.4% could be obtained after 120 s contrarily to 64.6 and 66.6% for BFA and TF-BFA (See Figure 18). This is directly related to the ability of CC-TFA to produce twice more radicals. Noticeably, during the FRP of TMPTA, similar conversions could be obtained with the three derivatives (around 53%) and this result was assigned to the higher viscosity of TMPTA and the trifunctional character of the monomer speeding up the gelation process and adversely the double bond conversion. However, these monomer conversions remain lower than those previously obtained with DM-BD-F, with conversions of 79.1 and 46.8 being respectively obtained during the FRP of TPGDA and TMPTA.

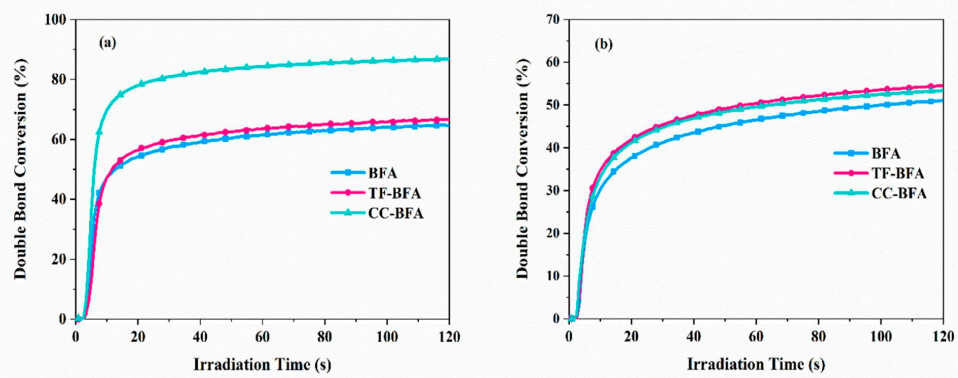

Figure 18. Photopolymerization profiles of (**a**) TPGDA and (**b**) TMPTA in laminate using BFAs (1.10^{-4} mol/g monomer) upon irradiation at 405 nm with a LED. Reproduced with the permission of Ref. [240]. Copyright 2022. Elsevier.

A similar trend was determined during the FRP of a water-soluble monomer, namely PEG diacrylate (PEGDA). Upon irradiation at 405 nm and by performing the polymerization experiments in water, a conversion of ca. 80% could be obtained within 180 s (see Figure 19). Besides, a slower polymerization rate could be evidenced for CC-BFA, resulting from its poor water solubility.

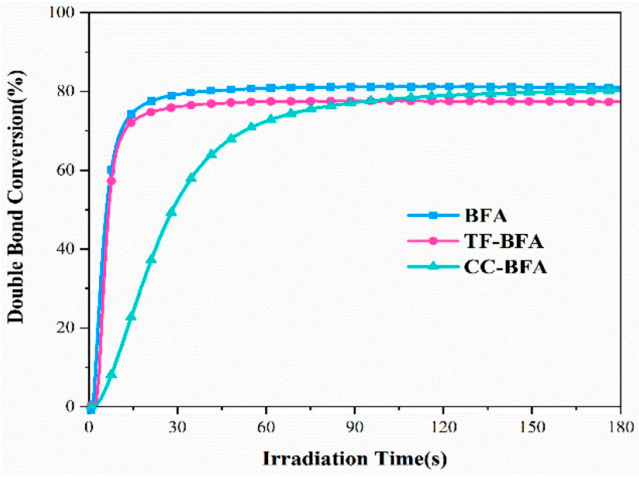

Figure 19. Photopolymerization profiles of PEGDA in laminate using BFAs (1×10^{-4} mol/g monomer) upon irradiation at 405 nm with a LED. Reproduced with the permission of Ref. [240]. Copyright 2022. Elsevier.

Water solubility tests revealed the water solubility of BFA and TF-BFA to be between 10 and 5 wt%. Conversely, this value was reduced to only 0.5 wt% for CC-TFA, despites the present of two carboxylic acid groups. This counter-intuitive result was assigned to the absence of dipole moment in CC-TFA, affecting its solubility in high polar media. Finally, an investigation of the curing depth in PEGDA revealed BFA and TF-BFA to give a similar curing depth (6.3 cm and 6.7 cm respectively). This value is higher than that obtained with BAPO (only 1 cm). Additionally, colorless polymers could be obtained, which is highly worthwhile for future applications of these structures.

2.5. Cytotoxicity of Glyoxylates

If polymerization efficiency is an important parameter governing the choice of photoinitiators, their toxicity is another major issue as it drastically impacts the scope of applications of polymers. Indeed, for biomedical applications or food packaging, the use of photoinitiators exhibiting low toxicity is required. This point was examined with a series of seven benchmark photoinitiators including methyl benzoylformate (MBF) (see Figure 20) [241].

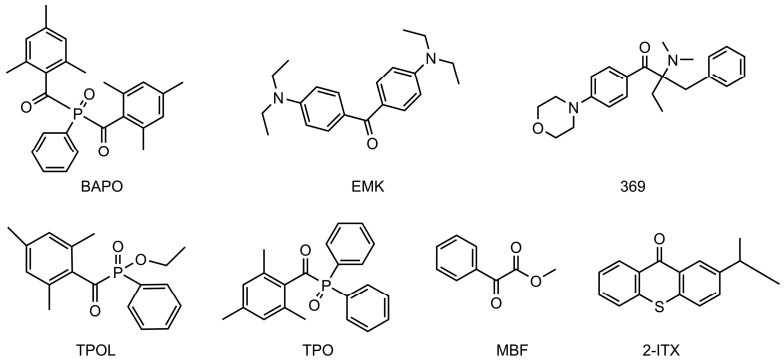

Figure 20. Chemical structures of seven benchmark photoinitiators were investigated for their cytotoxicity. Reproduced with the permission of Ref. [241]. Copyright 2021. Elsevier.

Cytotoxicity tests carried out on four different tissue types of cells at concentrations ranging between 1 and 50 µM revealed phenylbis(acyl)phosphine oxide (BAPO), 2-benzyl-2-(dimethylamino)-4′-morpholinobutyrophenone (369), 4,4′-*bis*(diethylamino)benzophenone (EMK), diphenyl (2,4,6-trimethylbenzoyl)phosphine oxide (TPO), and 2-isopropylthioxanthone (ITX) to be more toxic than ethyl (2,4,6-trimethylbenzoyl)phenylphosphinate (TPOL) and methyl benzoylformate (MBF). In this series of photoinitiators, the most toxic structure was identified as BAPO, which is extensively used in industry. In the case of TPOL and MBF, the less toxic structure was identified as being TPOL. These different results can help for future developments of new photoinitiators in light of the low cytotoxicity of MBF.

3. Conclusions

To conclude, glyoxylates and related structures have only been scarcely investigated in the literature. The different results obtained with these structures are promising. As the first point, low cytotoxicity should be highlighted, which constitutes a clear advantage for future applications of polymers. Water-soluble dyes could also be prepared, enabling the polymerization in water. Furthermore, to keep a good solubility in water, the molecule should exhibit a dipole moment to facilitate its dissolution. Glyoxylates and related structures can also operate as mono-component systems, greatly simplifying the composition of the photocurable resins. Excellent depths of cure and colorless coatings could also be obtained, evidencing the interest in these structures. At present, absorption of these structures remains strongly UV-centered. Future works will certainly consist of redshifting their absorption towards the visible range to further improve the depth of cure as well as the polymerization kinetics.

Funding: Aix Marseille University and the Centre National de la Recherche Scientifique are acknowledged for financial support under the frame of permanent funding.

Data Availability Statement: No data are available for this review.

Conflicts of Interest: The authors declare no conflict of interest.

References

1. Xiao, P.; Zhang, J.; Dumur, F.; Tehfe, M.A.; Morlet-Savary, F.; Graff, B.; Gigmes, D.; Fouassier, J.P.; Lalevée, J. Visible Light Sensitive Photoinitiating Systems: Recent Progress in Cationic and Radical Photopolymerization Reactions under Soft Conditions. *Prog. Polym. Sci.* **2015**, *41*, 32–66. [CrossRef]
2. Allegrezza, M.L.; DeMartini, Z.M.; Kloster, A.J.; Digby, Z.A.; Konkolewicz, D. Visible and Sunlight Driven RAFT Photopolymerization Accelerated by Amines: Kinetics and Mechanism. *Polym. Chem.* **2016**, *7*, 6626–6636. [CrossRef]
3. Sun, K.; Chen, H.; Zhang, Y.; Morlet-Savary, F.; Graff, B.; Xiao, P.; Dumur, F.; Lalevée, J. High-Performance Sunlight Induced Polymerization Using Novel Push-Pull Dyes with High Light Absorption Properties. *Eur. Polym. J.* **2021**, *151*, 110410. [CrossRef]
4. Sun, K.; Pigot, C.; Zhang, Y.; Borjigin, T.; Morlet-Savary, F.; Graff, B.; Nechab, M.; Xiao, P.; Dumur, F.; Lalevée, J. Sunlight Induced Polymerization Photoinitiated by Novel Push–Pull Dyes: Indane-1,3-Dione, 1H-Cyclopenta[b]Naphthalene-1,3(2H)-Dione and 4-Dimethoxyphenyl-1-Allylidene Derivatives. *Macromol. Chem. Phys.* **2022**, *223*, 2100439. [CrossRef]
5. Ciftci, M.; Tasdelen, M.A.; Yagci, Y. Sunlight Induced Atom Transfer Radical Polymerization by Using Dimanganese Decacarbonyl. *Polym. Chem.* **2014**, *5*, 600–606. [CrossRef]
6. Decker, C.; Bendaikha, T. Interpenetrating Polymer Networks. II. Sunlight-Induced Polymerization of Multifunctional Acrylates. *J. Appl. Polym. Sci.* **1998**, *70*, 2269–2282. [CrossRef]
7. Tehfe, M.-A.; Lalevée, J.; Gigmes, D.; Fouassier, J.P. Green Chemistry: Sunlight-Induced Cationic Polymerization of Renewable Epoxy Monomers Under Air. *Macromolecules* **2010**, *43*, 1364–1370. [CrossRef]
8. Wang, J.; Rivero, M.; Muñoz Bonilla, A.; Sanchez-Marcos, J.; Xue, W.; Chen, G.; Zhang, W.; Zhu, X. Natural RAFT Polymerization: Recyclable-Catalyst-Aided, Opened-to-Air, and Sunlight-Photolyzed RAFT Polymerizations. *ACS Macro Lett.* **2016**, *5*, 1278–1282. [CrossRef]
9. Yu, J.; Gao, Y.; Jiang, S.; Sun, F. Naphthalimide Aryl Sulfide Derivative Norrish Type I Photoinitiators with Excellent Stability to Sunlight under Near-UV LED. *Macromolecules* **2019**, *52*, 1707–1717. [CrossRef]
10. Armstrong, B.K.; Kricker, A. The Epidemiology of UV Induced Skin Cancer. *J. Photochem. Photobiol. B Biol.* **2001**, *63*, 8–18. [CrossRef]
11. de Gruijl, F.R. Skin Cancer and Solar UV Radiation. *Eur. J. Cancer* **1999**, *35*, 2003–2009. [CrossRef] [PubMed]
12. Jasinski, F.; Zetterlund, P.B.; Braun, A.M.; Chemtob, A. Photopolymerization in Dispersed Systems. *Prog. Polym. Sci.* **2018**, *84*, 47–88. [CrossRef]
13. Noè, C.; Hakkarainen, M.; Sangermano, M. Cationic UV-Curing of Epoxidized Biobased Resins. *Polymers* **2021**, *13*, 89. [CrossRef]
14. Yuan, Y.; Li, C.; Zhang, R.; Liu, R.; Liu, J. Low Volume Shrinkage Photopolymerization System Using Hydrogen-Bond-Based Monomers. *Prog. Org. Coat.* **2019**, *137*, 105308. [CrossRef]
15. Khudyakov, I.V.; Legg, J.C.; Purvis, M.B.; Overton, B.J. Kinetics of Photopolymerization of Acrylates with Functionality of 1−6. *Ind. Eng. Chem. Res.* **1999**, *38*, 3353–3359. [CrossRef]
16. Dickens, S.H.; Stansbury, J.W.; Choi, K.M.; Floyd, C.J.E. Photopolymerization Kinetics of Methacrylate Dental Resins. *Macromolecules* **2003**, *36*, 6043–6053. [CrossRef]
17. Maffezzoli, A.; Pietra, A.D.; Rengo, S.; Nicolais, L.; Valletta, G. Photopolymerization of Dental Composite Matrices. *Biomaterials* **1994**, *15*, 1221–1228. [CrossRef]
18. Dikova, T.; Maximov, J.; Todorov, V.; Georgiev, G.; Panov, V. Optimization of Photopolymerization Process of Dental Composites. *Processes* **2021**, *9*, 779. [CrossRef]
19. Andreu, A.; Su, P.-C.; Kim, J.-H.; Ng, C.S.; Kim, S.; Kim, I.; Lee, J.; Noh, J.; Subramanian, A.S.; Yoon, Y.-J. 4D Printing Materials for Vat Photopolymerization. *Addit. Manuf.* **2021**, *44*, 102024. [CrossRef]
20. Chen, H.; Noirbent, G.; Zhang, Y.; Sun, K.; Liu, S.; Brunel, D.; Gigmes, D.; Graff, B.; Morlet-Savary, F.; Xiao, P.; et al. Photopolymerization and 3D/4D Applications Using Newly Developed Dyes: Search around the Natural Chalcone Scaffold in Photoinitiating Systems. *Dyes Pigments* **2021**, *188*, 109213. [CrossRef]
21. Bagheri, A.; Jin, J. Photopolymerization in 3D Printing. *ACS Appl. Polym. Mater.* **2019**, *1*, 593–611. [CrossRef]
22. Fouassier, J.P.; Lalevée, J. Three-Component Photoinitiating Systems: Towards Innovative Tailor Made High Performance Combinations. *RSC Adv.* **2012**, *2*, 2621–2629. [CrossRef]
23. Lalevée, J.; Fouassier, J.-P. *Dyes and Chromophores in Polymer Science*; ISTE Ltd.: London, UK; John Wiley & Sons Inc.: Hoboken, NJ, USA, 2015; ISBN 978-1-84821-742-3.
24. Lalevée, J.; Telitel, S.; Xiao, P.; Lepeltier, M.; Dumur, F.; Morlet-Savary, F.; Gigmes, D.; Fouassier, J.-P. Metal and Metal-Free Photocatalysts: Mechanistic Approach and Application as Photoinitiators of Photopolymerization. *Beilstein J. Org. Chem.* **2014**, *10*, 863–876. [CrossRef] [PubMed]
25. Tomal, W.; Kiliclar, H.C.; Fiedor, P.; Ortyl, J.; Yagci, Y. Visible Light Induced High Resolution and Swift 3D Printing System by Halogen Atom Transfer. *Macromol. Rapid Commun.* **2023**, *44*, 2200661. [CrossRef]

26. Narayanan, D.L.; Saladi, R.N.; Fox, J.L. Review: Ultraviolet Radiation and Skin Cancer. *Int. J. Dermatol.* **2010**, *49*, 978–986. [CrossRef]
27. Shao, J.; Huang, Y.; Fan, Q. Visible Light Initiating Systems for Photopolymerization: Status, Development and Challenges. *Polym. Chem.* **2014**, *5*, 4195–4210. [CrossRef]
28. Hola, E.; Fiedor, P.; Dzienia, A.; Ortyl, J. Visible-Light Amine Thioxanthone Derivatives as Photoredox Catalysts for Photopolymerization Processes. *ACS Appl. Polym. Mater.* **2021**, *3*, 5547–5558. [CrossRef]
29. Hola, E.; Pilch, M.; Ortyl, J. Thioxanthone Derivatives as a New Class of Organic Photocatalysts for Photopolymerisation Processes and the 3D Printing of Photocurable Resins under Visible Light. *Catalysts* **2020**, *10*, 903. [CrossRef]
30. Lago, M.A.; de Quirós, A.R.-B.; Sendón, R.; Bustos, J.; Nieto, M.T.; Paseiro, P. Photoinitiators: A Food Safety Review. *Food Addit. Contam. Part A* **2015**, *32*, 779–798. [CrossRef]
31. Hammoud, F.; Hijazi, A.; Schmitt, M.; Dumur, F.; Lalevée, J. A Review on Recently Proposed Oxime Ester Photoinitiators. *Eur. Polym. J.* **2023**, *188*, 111901. [CrossRef]
32. Sun, K.; Xiao, P.; Dumur, F.; Lalevée, J. Organic Dye-Based Photoinitiating Systems for Visible-Light-Induced Photopolymerization. *J. Polym. Sci.* **2021**, *59*, 1338–1389. [CrossRef]
33. Bonardi, A.H.; Dumur, F.; Grant, T.M.; Noirbent, G.; Gigmes, D.; Lessard, B.H.; Fouassier, J.-P.; Lalevée, J. High Performance Near-Infrared (NIR) Photoinitiating Systems Operating under Low Light Intensity and in the Presence of Oxygen. *Macromolecules* **2018**, *51*, 1314–1324. [CrossRef]
34. Garra, P.; Dietlin, C.; Morlet-Savary, F.; Dumur, F.; Gigmes, D.; Fouassier, J.-P.; Lalevée, J. Photopolymerization Processes of Thick Films and in Shadow Areas: A Review for the Access to Composites. *Polym. Chem.* **2017**, *8*, 7088–7101. [CrossRef]
35. Liu, S.; Chen, H.; Zhang, Y.; Sun, K.; Xu, Y.; Morlet-Savary, F.; Graff, B.; Noirbent, G.; Pigot, C.; Brunel, D.; et al. Monocomponent Photoinitiators Based on Benzophenone-Carbazole Structure for LED Photoinitiating Systems and Application on 3D Printing. *Polymers* **2020**, *12*, 1394. [CrossRef] [PubMed]
36. Xiao, P.; Dumur, F.; Graff, B.; Gigmes, D.; Fouassier, J.P.; Lalevée, J. Variations on the Benzophenone Skeleton: Novel High Performance Blue Light Sensitive Photoinitiating Systems. *Macromolecules* **2013**, *46*, 7661–7667. [CrossRef]
37. Zhang, J.; Frigoli, M.; Dumur, F.; Xiao, P.; Ronchi, L.; Graff, B.; Morlet-Savary, F.; Fouassier, J.P.; Gigmes, D.; Lalevée, J. Design of Novel Photoinitiators for Radical and Cationic Photopolymerizations under Near UV and Visible LEDs (385, 395, and 405 Nm). *Macromolecules* **2014**, *47*, 2811–2819. [CrossRef]
38. Liu, S.; Brunel, D.; Noirbent, G.; Mau, A.; Chen, H.; Morlet-Savary, F.; Graff, B.; Gigmes, D.; Xiao, P.; Dumur, F.; et al. New Multifunctional Benzophenone-Based Photoinitiators with High Migration Stability and Their Applications in 3D Printing. *Mater. Chem. Front.* **2021**, *5*, 1982–1994. [CrossRef]
39. Liu, S.; Brunel, D.; Sun, K.; Zhang, Y.; Chen, H.; Xiao, P.; Dumur, F.; Lalevée, J. Novel Photoinitiators Based on Benzophenone-Triphenylamine Hybrid Structure for LED Photopolymerization. *Macromol. Rapid Commun.* **2020**, *41*, 2000460. [CrossRef]
40. Liu, S.; Brunel, D.; Sun, K.; Xu, Y.; Morlet-Savary, F.; Graff, B.; Xiao, P.; Dumur, F.; Lalevée, J. A Monocomponent Bifunctional Benzophenone–Carbazole Type II Photoinitiator for LED Photoinitiating Systems. *Polym. Chem.* **2020**, *11*, 3551–3556. [CrossRef]
41. Tehfe, M.-A.; Dumur, F.; Graff, B.; Morlet-Savary, F.; Fouassier, J.-P.; Gigmes, D.; Lalevée, J. Trifunctional Photoinitiators Based on a Triazine Skeleton for Visible Light Source and UV LED Induced Polymerizations. *Macromolecules* **2012**, *45*, 8639–8647. [CrossRef]
42. Lin, J.-T.; Lalevee, J. Efficacy Modeling of New Multi-Functional Benzophenone-Based System for Free-Radical/Cationic Hybrid Photopolymerization Using 405 Nm LED. *J. Polym. Res.* **2022**, *29*, 100. [CrossRef]
43. Topa-Skwarczyńska, M.; Galek, M.; Jankowska, M.; Morlet-Savary, F.; Graff, B.; Lalevée, J.; Popielarz, R.; Ortyl, J. Development of the First Panchromatic BODIPY-Based One-Component Iodonium Salts for Initiating the Photopolymerization Processes. *Polym. Chem.* **2021**, *12*, 6873–6893. [CrossRef]
44. Karaca, N.; Ocal, N.; Arsu, N.; Jockusch, S. Thioxanthone-Benzothiophenes as Photoinitiator for Free Radical Polymerization. *J. Photochem. Photobiol. Chem.* **2016**, *331*, 22–28. [CrossRef]
45. Balta, D.K.; Cetiner, N.; Temel, G.; Turgut, Z.; Arsu, N. An Annelated Thioxanthone as a New Type II Initiator. *J. Photochem. Photobiol. Chem.* **2008**, *199*, 316–321. [CrossRef]
46. Balta, D.K.; Temel, G.; Goksu, G.; Ocal, N.; Arsu, N. Thioxanthone–Diphenyl Anthracene: Visible Light Photoinitiator. *Macromolecules* **2012**, *45*, 119–125. [CrossRef]
47. Dadashi-Silab, S.; Aydogan, C.; Yagci, Y. Shining a Light on an Adaptable Photoinitiator: Advances in Photopolymerizations Initiated by Thioxanthones. *Polym. Chem.* **2015**, *6*, 6595–6615. [CrossRef]
48. Eren, T.N.; Yasar, N.; Aviyente, V.; Morlet-Savary, F.; Graff, B.; Fouassier, J.P.; Lalevee, J.; Avci, D. Photophysical and Photochemical Studies of Novel Thioxanthone-Functionalized Methacrylates through LED Excitation. *Macromol. Chem. Phys.* **2016**, *217*, 1501–1512. [CrossRef]
49. Qiu, J.; Wei, J. Thioxanthone Photoinitiator Containing Polymerizable N-Aromatic Maleimide for Photopolymerization. *J. Polym. Res.* **2014**, *21*, 559. [CrossRef]
50. Tar, H.; Sevinc Esen, D.; Aydin, M.; Ley, C.; Arsu, N.; Allonas, X. Panchromatic Type II Photoinitiator for Free Radical Polymerization Based on Thioxanthone Derivative. *Macromolecules* **2013**, *46*, 3266–3272. [CrossRef]
51. Wu, Q.; Wang, X.; Xiong, Y.; Yang, J.; Tang, H. Thioxanthone Based One-Component Polymerizable Visible Light Photoinitiator for Free Radical Polymerization. *RSC Adv.* **2016**, *6*, 66098–66107. [CrossRef]

52. Wu, Q.; Tang, K.; Xiong, Y.; Wang, X.; Yang, J.; Tang, H. High-Performance and Low Migration One-Component Thioxanthone Visible Light Photoinitiators. *Macromol. Chem. Phys.* **2017**, *218*, 1600484. [CrossRef]
53. Wu, X.; Jin, M.; Malval, J.-P.; Wan, D.; Pu, H. Visible Light-Emitting Diode-Sensitive Thioxanthone Derivatives Used in Versatile Photoinitiating Systems for Photopolymerizations. *J. Polym. Sci. Part Polym. Chem.* **2017**, *55*, 4037–4045. [CrossRef]
54. Lalevée, J.; Tehfe, M.-A.; Dumur, F.; Gigmes, D.; Graff, B.; Morlet-Savary, F.; Fouassier, J.-P. Light-Harvesting Organic Photoinitiators of Polymerization. *Macromol. Rapid Commun.* **2013**, *34*, 239–245. [CrossRef] [PubMed]
55. Esen, D.S.; Karasu, F.; Arsu, N. The Investigation of Photoinitiated Polymerization of Multifunctional Acrylates with TX-BT by Photo-DSC and RT-FTIR. *Prog. Org. Coat.* **2011**, *70*, 102–107. [CrossRef]
56. Lalevée, J.; Blanchard, N.; Tehfe, M.A.; Fries, C.; Morlet-Savary, F.; Gigmes, D.; Fouassier, J.P. New Thioxanthone and Xanthone Photoinitiators Based on Silyl Radical Chemistry. *Polym. Chem.* **2011**, *2*, 1077–1084. [CrossRef]
57. Gencoglu, T.; Eren, T.N.; Lalevée, J.; Avci, D. A Water Soluble, Low Migration, and Visible Light Photoinitiator by Thioxanthone-Functionalization of Poly(Ethylene Glycol)-Containing Poly(β-Amino Ester). *Macromol. Chem. Phys.* **2022**, *223*, 2100450. [CrossRef]
58. Wang, Y.; Chen, R.; Liu, D.; Peng, C.; Wang, J.; Dong, X. New Functionalized Thioxanthone Derivatives as Type I Photoinitiators for Polymerization under UV-Vis LEDs. *N. J. Chem.* **2023**, *47*, 5330–5337. [CrossRef]
59. Kamoun, E.A.; Winkel, A.; Eisenburger, M.; Menzel, H. Carboxylated Camphorquinone as Visible-Light Photoinitiator for Biomedical Application: Synthesis, Characterization, and Application. *Arab. J. Chem.* **2016**, *9*, 745–754. [CrossRef]
60. Santini, A.; Gallegos, I.T.; Felix, C.M. Photoinitiators in Dentistry: A Review. *Prim. Dent. J.* **2013**, *2*, 30–33. [CrossRef]
61. Zhao, J.; Lalevée, J.; Lu, H.; MacQueen, R.; Kable, S.H.; Schmidt, T.W.; Stenzel, M.H.; Xiao, P. A New Role of Curcumin: As a Multicolor Photoinitiator for Polymer Fabrication under Household UV to Red LED Bulbs. *Polym. Chem.* **2015**, *6*, 5053–5061. [CrossRef]
62. Crivello, J.V.; Bulut, U. Curcumin: A Naturally Occurring Long-Wavelength Photosensitizer for Diaryliodonium Salts. *J. Polym. Sci. Part Polym. Chem.* **2005**, *43*, 5217–5231. [CrossRef]
63. Han, W.; Fu, H.; Xue, T.; Liu, T.; Wang, Y.; Wang, T. Facilely Prepared Blue-Green Light Sensitive Curcuminoids with Excellent Bleaching Properties as High Performance Photosensitizers in Cationic and Free Radical Photopolymerization. *Polym. Chem.* **2018**, *9*, 1787–1798. [CrossRef]
64. Mishra, A.; Daswal, S. Curcumin, A Novel Natural Photoinitiator for the Copolymerization of Styrene and Methylmethacrylate. *J. Macromol. Sci. Part A* **2005**, *42*, 1667–1678. [CrossRef]
65. Tehfe, M.-A.; Dumur, F.; Xiao, P.; Graff, B.; Morlet-Savary, F.; Fouassier, J.-P.; Gigmes, D.; Lalevée, J. New Chromone Based Photoinitiators for Polymerization Reactions under Visible Light. *Polym. Chem.* **2013**, *4*, 4234–4244. [CrossRef]
66. You, J.; Fu, H.; Zhao, D.; Hu, T.; Nie, J.; Wang, T. Flavonol Dyes with Different Substituents in Photopolymerization. *J. Photochem. Photobiol. Chem.* **2020**, *386*, 112097. [CrossRef]
67. Al Mousawi, A.; Garra, P.; Schmitt, M.; Toufaily, J.; Hamieh, T.; Graff, B.; Fouassier, J.P.; Dumur, F.; Lalevée, J. 3-Hydroxyflavone and N-Phenylglycine in High Performance Photoinitiating Systems for 3D Printing and Photocomposites Synthesis. *Macromolecules* **2018**, *51*, 4633–4641. [CrossRef]
68. Tehfe, M.-A.; Dumur, F.; Contal, E.; Graff, B.; Gigmes, D.; Fouassier, J.-P.; Lalevée, J. Novel Highly Efficient Organophotocatalysts: Truxene–Acridine-1,8-Diones as Photoinitiators of Polymerization. *Macromol. Chem. Phys.* **2013**, *214*, 2189–2201. [CrossRef]
69. Xiao, P.; Dumur, F.; Tehfe, M.-A.; Graff, B.; Gigmes, D.; Fouassier, J.P.; Lalevée, J. Difunctional Acridinediones as Photoinitiators of Polymerization under UV and Visible Lights: Structural Effects. *Polymer* **2013**, *54*, 3458–3466. [CrossRef]
70. Abdallah, M.; Le, H.; Hijazi, A.; Schmitt, M.; Graff, B.; Dumur, F.; Bui, T.-T.; Goubard, F.; Fouassier, J.-P.; Lalevée, J. Acridone Derivatives as High Performance Visible Light Photoinitiators for Cationic and Radical Photosensitive Resins for 3D Printing Technology and for Low Migration Photopolymer Property. *Polymer* **2018**, *159*, 47–58. [CrossRef]
71. Tehfe, M.-A.; Dumur, F.; Contal, E.; Graff, B.; Morlet-Savary, F.; Gigmes, D.; Fouassier, J.-P.; Lalevée, J. New Insights into Radical and Cationic Polymerizations upon Visible Light Exposure: Role of Novel Photoinitiator Systems Based on the Pyrene Chromophore. *Polym. Chem.* **2013**, *4*, 1625–1634. [CrossRef]
72. Telitel, S.; Dumur, F.; Faury, T.; Graff, B.; Tehfe, M.-A.; Gigmes, D.; Fouassier, J.-P.; Lalevée, J. New Core-Pyrene π Structure Organophotocatalysts Usable as Highly Efficient Photoinitiators. *Beilstein J. Org. Chem.* **2013**, *9*, 877–890. [CrossRef] [PubMed]
73. Uchida, N.; Nakano, H.; Igarashi, T.; Sakurai, T. Nonsalt 1-(Arylmethyloxy)Pyrene Photoinitiators Capable of Initiating Cationic Polymerization. *J. Appl. Polym. Sci.* **2014**, *131*, 40510. [CrossRef]
74. Mishra, A.; Daswal, S. 1-(Bromoacetyl)Pyrene, a Novel Photoinitiator for the Copolymerization of Styrene and Methylmethacrylate. *Radiat. Phys. Chem.* **2006**, *75*, 1093–1100. [CrossRef]
75. Tehfe, M.-A.; Dumur, F.; Graff, B.; Morlet-Savary, F.; Gigmes, D.; Fouassier, J.-P.; Lalevée, J. Design of New Type I and Type II Photoinitiators Possessing Highly Coupled Pyrene–Ketone Moieties. *Polym. Chem.* **2013**, *4*, 2313–2324. [CrossRef]
76. Dumur, F. Recent Advances on Pyrene-Based Photoinitiators of Polymerization. *Eur. Polym. J.* **2020**, *126*, 109564. [CrossRef]
77. Tehfe, M.-A.; Dumur, F.; Vilà, N.; Graff, B.; Mayer, C.R.; Fouassier, J.P.; Gigmes, D.; Lalevée, J. A Multicolor Photoinitiator for Cationic Polymerization and Interpenetrated Polymer Network Synthesis: 2,7-Di-Tert-Butyldimethyldihydropyrene. *Macromol. Rapid Commun.* **2013**, *34*, 1104–1109. [CrossRef]
78. Telitel, S.; Dumur, F.; Gigmes, D.; Graff, B.; Fouassier, J.P.; Lalevée, J. New Functionalized Aromatic Ketones as Photoinitiating Systems for near Visible and Visible Light Induced Polymerizations. *Polymer* **2013**, *54*, 2857–2864. [CrossRef]

79. Tehfe, M.-A.; Lalevée, J.; Telitel, S.; Contal, E.; Dumur, F.; Gigmes, D.; Bertin, D.; Nechab, M.; Graff, B.; Morlet-Savary, F.; et al. Polyaromatic Structures as Organo-Photoinitiator Catalysts for Efficient Visible Light Induced Dual Radical/Cationic Photopolymerization and Interpenetrated Polymer Networks Synthesis. *Macromolecules* **2012**, *45*, 4454–4460. [CrossRef]
80. Dumur, F. Recent Advances on Anthracene-Based Photoinitiators of Polymerization. *Eur. Polym. J.* **2022**, *169*, 111139. [CrossRef]
81. Zhang, J.; Campolo, D.; Dumur, F.; Xiao, P.; Gigmes, D.; Fouassier, J.P.; Lalevée, J. The Carbazole-Bound Ferrocenium Salt as a Specific Cationic Photoinitiator upon near-UV and Visible LEDs (365–405 Nm). *Polym. Bull.* **2016**, *73*, 493–507. [CrossRef]
82. Al Mousawi, A.; Dumur, F.; Garra, P.; Toufaily, J.; Hamieh, T.; Graff, B.; Gigmes, D.; Fouassier, J.P.; Lalevée, J. Carbazole Scaffold Based Photoinitiator/Photoredox Catalysts: Toward New High Performance Photoinitiating Systems and Application in LED Projector 3D Printing Resins. *Macromolecules* **2017**, *50*, 2747–2758. [CrossRef]
83. Al Mousawi, A.; Lara, D.M.; Noirbent, G.; Dumur, F.; Toufaily, J.; Hamieh, T.; Bui, T.-T.; Goubard, F.; Graff, B.; Gigmes, D.; et al. Carbazole Derivatives with Thermally Activated Delayed Fluorescence Property as Photoinitiators/Photoredox Catalysts for LED 3D Printing Technology. *Macromolecules* **2017**, *50*, 4913–4926. [CrossRef]
84. Al Mousawi, A.; Garra, P.; Dumur, F.; Bui, T.-T.; Goubard, F.; Toufaily, J.; Hamieh, T.; Graff, B.; Gigmes, D.; Fouassier, J.P.; et al. Novel Carbazole Skeleton-Based Photoinitiators for LED Polymerization and LED Projector 3D Printing. *Molecules* **2017**, *22*, 2143. [CrossRef] [PubMed]
85. Mousawi, A.A.; Arar, A.; Ibrahim-Ouali, M.; Duval, S.; Dumur, F.; Garra, P.; Toufaily, J.; Hamieh, T.; Graff, B.; Gigmes, D.; et al. Carbazole-Based Compounds as Photoinitiators for Free Radical and Cationic Polymerization upon near Visible Light Illumination. *Photochem. Photobiol. Sci.* **2018**, *17*, 578–585. [CrossRef]
86. Abdallah, M.; Magaldi, D.; Hijazi, A.; Graff, B.; Dumur, F.; Fouassier, J.-P.; Bui, T.-T.; Goubard, F.; Lalevée, J. Development of New High-Performance Visible Light Photoinitiators Based on Carbazole Scaffold and Their Applications in 3d Printing and Photocomposite Synthesis. *J. Polym. Sci. Part Polym. Chem.* **2019**, *57*, 2081–2092. [CrossRef]
87. Dumur, F. Recent Advances on Carbazole-Based Photoinitiators of Polymerization. *Eur. Polym. J.* **2020**, *125*, 109503. [CrossRef]
88. Liu, S.; Graff, B.; Xiao, P.; Dumur, F.; Lalevée, J. Nitro-Carbazole Based Oxime Esters as Dual Photo/Thermal Initiators for 3D Printing and Composite Preparation. *Macromol. Rapid Commun.* **2021**, *42*, 2100207. [CrossRef]
89. Hammoud, F.; Hijazi, A.; Duval, S.; Lalevée, J.; Dumur, F. 5,12-Dihydroindolo[3,2-a]Carbazole: A Promising Scaffold for the Design of Visible Light Photoinitiators of Polymerization. *Eur. Polym. J.* **2022**, *162*, 110880. [CrossRef]
90. Liu, S.; Giacoletto, N.; Schmitt, M.; Nechab, M.; Graff, B.; Morlet-Savary, F.; Xiao, P.; Dumur, F.; Lalevée, J. Effect of Decarboxylation on the Photoinitiation Behavior of Nitrocarbazole-Based Oxime Esters. *Macromolecules* **2022**, *55*, 2475–2485. [CrossRef]
91. Hammoud, F.; Hijazi, A.; Ibrahim-Ouali, M.; Lalevée, J.; Dumur, F. Chemical Engineering around the 5,12-Dihydroindolo[3,2-a]Carbazole Scaffold: Fine Tuning of the Optical Properties of Visible Light Photoinitiators of Polymerization. *Eur. Polym. J.* **2022**, *172*, 111218. [CrossRef]
92. Xu, C.; Gong, S.; Wu, X.; Wu, Y.; Liao, Q.; Xiong, Y.; Li, Z.; Tang, H. High-Efficient Carbazole-Based Photo-Bleachable Dyes as Free Radical Initiators for Visible Light Polymerization. *Dye. Pigment.* **2022**, *198*, 110039. [CrossRef]
93. Dumur, F. Recent Advances on Carbazole-Based Oxime Esters as Photoinitiators of Polymerization. *Eur. Polym. J.* **2022**, *175*, 111330. [CrossRef]
94. Hammoud, F.; Giacoletto, N.; Nechab, M.; Graff, B.; Hijazi, A.; Dumur, F.; Lalevée, J. 5,12-Dialkyl-5,12-Dihydroindolo[3,2-a]Carbazole-Based Oxime-Esters for LED Photoinitiating Systems and Application on 3D Printing. *Macromol. Mater. Eng.* **2022**, *307*, 2200082. [CrossRef]
95. Liao, W.; Liao, Q.; Xiong, Y.; Li, Z.; Tang, H. Design, Synthesis and Properties of Carbazole-Indenedione Based Photobleachable Photoinitiators for Photopolymerization. *J. Photochem. Photobiol. Chem.* **2023**, *435*, 114297. [CrossRef]
96. Bin, F.-C.; Guo, M.; Li, T.; Zheng, Y.-C.; Dong, X.-Z.; Liu, J.; Jin, F.; Zheng, M.-L. Carbazole-Based Anion Ionic Water-Soluble Two-Photon Initiator for Achieving 3D Hydrogel Structures. *Adv. Funct. Mater.* **2023**, 2300293. [CrossRef]
97. Bao, B.; You, J.; Li, D.; Zhan, H.; Zhang, L.; Li, M.; Wang, T. Double Benzylidene Ketones as Photoinitiators for Visible Light Photopolymerization. *J. Photochem. Photobiol. Chem.* **2022**, *429*, 113938. [CrossRef]
98. Fu, H.; Qiu, Y.; You, J.; Hao, T.; Fan, B.; Nie, J.; Wang, T. Photopolymerization of Acrylate Resin and Ceramic Suspensions with Benzylidene Ketones under Blue/Green LED. *Polymer* **2019**, *184*, 121841. [CrossRef]
99. Dumur, F. Recent Advances on Benzylidene Ketones as Photoinitiators of Polymerization. *Eur. Polym. J.* **2022**, *178*, 111500. [CrossRef]
100. Zhao, Y.; Wang, W.; Wu, F.; Zhou, Y.; Huang, N.; Gu, Y.; Zou, Q.; Yang, W. Polyethylene Glycol-Functionalized Benzylidene Cyclopentanone Dyes for Two-Photon Excited Photodynamic Therapy. *Org. Biomol. Chem.* **2011**, *9*, 4168–4175. [CrossRef]
101. Fang, Y.; Liu, T.; Zou, Q.; Zhao, Y.; Wu, F. Cationic Benzylidene Cyclopentanone Photosensitizers for Selective Photodynamic Inactivation of Bacteria over Mammalian Cells. *RSC Adv.* **2015**, *5*, 56067–56074. [CrossRef]
102. Xue, J.; Zhao, Y.; Wu, F.; Fang, D.-C. Effect of Bridging Position on the Two-Photon Polymerization Initiating Efficiencies of Novel Coumarin/Benzylidene Cyclopentanone Dyes. *J. Phys. Chem. A* **2010**, *114*, 5171–5179. [CrossRef] [PubMed]
103. Dumur, F. Recent Advances on Benzylidene Cyclopentanones as Visible Light Photoinitiators of Polymerization. *Eur. Polym. J.* **2022**, *181*, 111639. [CrossRef]
104. Egorov, A.E.; Kostyukov, A.A.; Shcherbakov, D.A.; Kolymagin, D.A.; Chubich, D.A.; Matital, R.P.; Arsenyev, M.V.; Burtsev, I.D.; Mestergazi, M.G.; Zhiganshina, E.R.; et al. Benzylidene Cyclopentanone Derivative Photoinitiator for Two-Photon Photopolymerization-Photochemistry and 3D Structures Fabrication for X-Ray Application. *Polymers* **2023**, *15*, 71. [CrossRef]

105. Li, J.; Zhang, X.; Ali, S.; Akram, M.Y.; Nie, J.; Zhu, X. The Effect of Polyethylene Glycoldiacrylate Complexation on Type II Photoinitiator and Promotion for Visible Light Initiation System. *J. Photochem. Photobiol. Chem.* **2019**, *384*, 112037. [CrossRef]
106. Li, J.; Li, S.; Li, Y.; Li, R.; Nie, J.; Zhu, X. In Situ Monitoring of Photopolymerization by Photoinitiator with Luminescence Characteristics. *J. Photochem. Photobiol. Chem.* **2020**, *389*, 112225. [CrossRef]
107. Li, J.; Hao, Y.; Zhong, M.; Tang, L.; Nie, J.; Zhu, X. Synthesis of Furan Derivative as LED Light Photoinitiator: One-Pot, Low Usage, Photobleaching for Light Color 3D Printing. *Dye. Pigment.* **2019**, *165*, 467–473. [CrossRef]
108. Xu, Y.; Noirbent, G.; Brunel, D.; Ding, Z.; Gigmes, D.; Graff, B.; Xiao, P.; Dumur, F.; Lalevée, J. Novel Ketone Derivative-Based Photoinitiating Systems for Free Radical Polymerization under Mild Conditions and 3D Printing. *Polym. Chem.* **2020**, *11*, 5767–5777. [CrossRef]
109. Chen, H.; Noirbent, G.; Sun, K.; Brunel, D.; Gigmes, D.; Morlet-Savary, F.; Zhang, Y.; Liu, S.; Xiao, P.; Dumur, F.; et al. Photoinitiators Derived from Natural Product Scaffolds: Monochalcones in Three-Component Photoinitiating Systems and Their Applications in 3D Printing. *Polym. Chem.* **2020**, *11*, 4647–4659. [CrossRef]
110. Tang, L.; Nie, J.; Zhu, X. A High Performance Phenyl-Free LED Photoinitiator for Cationic or Hybrid Photopolymerization and Its Application in LED Cationic 3D Printing. *Polym. Chem.* **2020**, *11*, 2855–2863. [CrossRef]
111. Xu, Y.; Noirbent, G.; Brunel, D.; Ding, Z.; Gigmes, D.; Graff, B.; Xiao, P.; Dumur, F.; Lalevée, J. Allyloxy Ketones as Efficient Photoinitiators with High Migration Stability in Free Radical Polymerization and 3D Printing. *Dye. Pigment.* **2021**, *185*, 108900. [CrossRef]
112. Xu, Y.; Ding, Z.; Zhu, H.; Graff, B.; Knopf, S.; Xiao, P.; Dumur, F.; Lalevée, J. Design of Ketone Derivatives as Highly Efficient Photoinitiators for Free Radical and Cationic Photopolymerizations and Application in 3D Printing of Composites. *J. Polym. Sci.* **2020**, *58*, 3432–3445. [CrossRef]
113. Chen, H.; Noirbent, G.; Liu, S.; Brunel, D.; Graff, B.; Gigmes, D.; Zhang, Y.; Sun, K.; Morlet-Savary, F.; Xiao, P.; et al. Bis-Chalcone Derivatives Derived from Natural Products as near-UV/Visible Light Sensitive Photoinitiators for 3D/4D Printing. *Mater. Chem. Front.* **2021**, *5*, 901–916. [CrossRef]
114. Liu, S.; Zhang, Y.; Sun, K.; Graff, B.; Xiao, P.; Dumur, F.; Lalevée, J. Design of Photoinitiating Systems Based on the Chalcone-Anthracene Scaffold for LED Cationic Photopolymerization and Application in 3D Printing. *Eur. Polym. J.* **2021**, *147*, 110300. [CrossRef]
115. Giacoletto, N.; Dumur, F. Recent Advances in Bis-Chalcone-Based Photoinitiators of Polymerization: From Mechanistic Investigations to Applications. *Molecules* **2021**, *26*, 3192. [CrossRef]
116. Ibrahim-Ouali, M.; Dumur, F. Recent Advances on Chalcone-Based Photoinitiators of Polymerization. *Eur. Polym. J.* **2021**, *158*, 110688. [CrossRef]
117. Chen, H.; Noirbent, G.; Liu, S.; Zhang, Y.; Sun, K.; Morlet-Savary, F.; Gigmes, D.; Xiao, P.; Dumur, F.; Lalevée, J. In Situ Generation of Ag Nanoparticles during Photopolymerization by Using Newly Developed Dyes-Based Three-Component Photoinitiating Systems and the Related 3D Printing Applications and Their Shape Change Behavior. *J. Polym. Sci.* **2021**, *59*, 843–859. [CrossRef]
118. Chen, H.; Vahdati, M.; Xiao, P.; Dumur, F.; Lalevée, J. Water-Soluble Visible Light Sensitive Photoinitiating System Based on Charge Transfer Complexes for the 3D Printing of Hydrogels. *Polymers* **2021**, *13*, 1395. [CrossRef]
119. Tehfe, M.-A.; Dumur, F.; Xiao, P.; Delgove, M.; Graff, B.; Fouassier, J.-P.; Gigmes, D.; Lalevée, J. Chalcone Derivatives as Highly Versatile Photoinitiators for Radical, Cationic, Thiol–Ene and IPN Polymerization Reactions upon Exposure to Visible Light. *Polym. Chem.* **2014**, *5*, 382–390. [CrossRef]
120. Sun, K.; Xu, Y.; Dumur, F.; Morlet-Savary, F.; Chen, H.; Dietlin, C.; Graff, B.; Lalevée, J.; Xiao, P. In Silico Rational Design by Molecular Modeling of New Ketones as Photoinitiators in Three-Component Photoinitiating Systems: Application in 3D Printing. *Polym. Chem.* **2020**, *11*, 2230–2242. [CrossRef]
121. Chen, H.; Regeard, C.; Salmi, H.; Morlet-Savary, F.; Giacoletto, N.; Nechab, M.; Xiao, P.; Dumur, F.; Lalevée, J. Interpenetrating Polymer Network Hydrogels Using Natural Based Dyes Initiating Systems: Antibacterial Activity and 3D/4D Performance. *Eur. Polym. J.* **2022**, *166*, 111042. [CrossRef]
122. Yen, S.-C.; Ni, J.-S.; Chen, Y.-C. Triphenylamine-Functionalized Chalcones as One-Component Type II Visible-Light-Absorbing Photoinitiators for Free Radical Photopolymerization. *Eur. Polym. J.* **2023**, *187*, 111885. [CrossRef]
123. Gao, Y.; Qu, J. New Long-Wavelength D–π-A–π-D Chalcone Photoinitiator for Visible Light Polymerization with Photobleaching and Biocompatibility Properties. *Polym. Chem.* **2023**, *14*, 952–962. [CrossRef]
124. Deng, L.; Qu, J. Synthesis and Properties of Novel Bis-Chalcone-Based Photoinitiators for LED Polymerization with Photobleaching and Low Migration. *Prog. Org. Coat.* **2023**, *174*, 107240. [CrossRef]
125. Mokbel, H.; Dumur, F.; Lalevée, J. On Demand NIR Activated Photopolyaddition Reactions. *Polym. Chem.* **2020**, *11*, 4250–4259. [CrossRef]
126. Mokbel, H.; Graff, B.; Dumur, F.; Lalevée, J. NIR Sensitizer Operating under Long Wavelength (1064 Nm) for Free Radical Photopolymerization Processes. *Macromol. Rapid Commun.* **2020**, *41*, 2000289. [CrossRef] [PubMed]
127. Launay, V.; Dumur, F.; Gigmes, D.; Lalevée, J. Near-Infrared Light for Polymer Re-Shaping and Re-Processing Applications. *J. Polym. Sci.* **2021**, *59*, 2193–2200. [CrossRef]
128. Caron, A.; Noirbent, G.; Gigmes, D.; Dumur, F.; Lalevée, J. Near-Infrared PhotoInitiating Systems: Photothermal versus Triplet–Triplet Annihilation-Based Upconversion Polymerization. *Macromol. Rapid Commun.* **2021**, *42*, 2100047. [CrossRef] [PubMed]

129. Bonardi, A.-H.; Bonardi, F.; Morlet-Savary, F.; Dietlin, C.; Noirbent, G.; Grant, T.M.; Fouassier, J.-P.; Dumur, F.; Lessard, B.H.; Gigmes, D.; et al. Photoinduced Thermal Polymerization Reactions. *Macromolecules* **2018**, *51*, 8808–8820. [CrossRef]
130. Launay, V.; Dumur, F.; Pieuchot, L.; Lalevée, J. Safe near Infrared Light for Fast Polymers Surface Sterilization Using Organic Heaters. *Mater. Chem. Front.* **2022**, *6*, 1172–1179. [CrossRef]
131. Launay, V.; Wolf, R.; Dumur, F.; Lalevée, J. Photothermal Activation in the near Infrared Range for 4-Dimensional Printing Using Relevant Organic Dyes. *Addit. Manuf.* **2022**, *58*, 103031. [CrossRef]
132. Garra, P.; Brunel, D.; Noirbent, G.; Graff, B.; Morlet-Savary, F.; Dietlin, C.; Sidorkin, V.F.; Dumur, F.; Duché, D.; Gigmes, D.; et al. Ferrocene-Based (Photo)Redox Polymerization under Long Wavelengths. *Polym. Chem.* **2019**, *10*, 1431–1441. [CrossRef]
133. Tehfe, M.-A.; Zein-Fakih, A.; Lalevée, J.; Dumur, F.; Gigmes, D.; Graff, B.; Morlet-Savary, F.; Hamieh, T.; Fouassier, J.-P. New Pyridinium Salts as Versatile Compounds for Dye Sensitized Photopolymerization. *Eur. Polym. J.* **2013**, *49*, 567–574. [CrossRef]
134. Xiao, P.; Frigoli, M.; Dumur, F.; Graff, B.; Gigmes, D.; Fouassier, J.P.; Lalevée, J. Julolidine or Fluorenone Based Push–Pull Dyes for Polymerization upon Soft Polychromatic Visible Light or Green Light. *Macromolecules* **2014**, *47*, 106–112. [CrossRef]
135. Mokbel, H.; Dumur, F.; Graff, B.; Mayer, C.R.; Gigmes, D.; Toufaily, J.; Hamieh, T.; Fouassier, J.-P.; Lalevée, J. Michler's Ketone as an Interesting Scaffold for the Design of High-Performance Dyes in Photoinitiating Systems Upon Visible Light. *Macromol. Chem. Phys.* **2014**, *215*, 783–790. [CrossRef]
136. Tehfe, M.-A.; Dumur, F.; Graff, B.; Morlet-Savary, F.; Fouassier, J.-P.; Gigmes, D.; Lalevée, J. New Push–Pull Dyes Derived from Michler's Ketone For Polymerization Reactions Upon Visible Lights. *Macromolecules* **2013**, *46*, 3761–3770. [CrossRef]
137. Mokbel, H.; Dumur, F.; Mayer, C.R.; Morlet-Savary, F.; Graff, B.; Gigmes, D.; Toufaily, J.; Hamieh, T.; Fouassier, J.-P.; Lalevée, J. End Capped Polyenic Structures as Visible Light Sensitive Photoinitiators for Polymerization of Vinylethers. *Dye. Pigment.* **2014**, *105*, 121–129. [CrossRef]
138. Telitel, S.; Dumur, F.; Kavalli, T.; Graff, B.; Morlet-Savary, F.; Gigmes, D.; Fouassier, J.-P.; Lalevée, J. The 1,3-Bis(Dicyanomethylidene)Indane Skeleton as a (Photo) Initiator in Thermal Ring Opening Polymerization at RT and Radical or Cationic Photopolymerization. *RSC Adv.* **2014**, *4*, 15930–15936. [CrossRef]
139. Xiao, P.; Dumur, F.; Graff, B.; Morlet-Savary, F.; Vidal, L.; Gigmes, D.; Fouassier, J.P.; Lalevée, J. Structural Effects in the Indanedione Skeleton for the Design of Low Intensity 300–500 Nm Light Sensitive Initiators. *Macromolecules* **2014**, *47*, 26–34. [CrossRef]
140. Sun, K.; Liu, S.; Pigot, C.; Brunel, D.; Graff, B.; Nechab, M.; Gigmes, D.; Morlet-Savary, F.; Zhang, Y.; Xiao, P.; et al. Novel Push–Pull Dyes Derived from 1H-Cyclopenta[b]Naphthalene-1,3(2H)-Dione as Versatile Photoinitiators for Photopolymerization and Their Related Applications: 3D Printing and Fabrication of Photocomposites. *Catalysts* **2020**, *10*, 1196. [CrossRef]
141. Sun, K.; Liu, S.; Chen, H.; Morlet-Savary, F.; Graff, B.; Pigot, C.; Nechab, M.; Xiao, P.; Dumur, F.; Lalevée, J. N-Ethyl Carbazole-1-Allylidene-Based Push-Pull Dyes as Efficient Light Harvesting Photoinitiators for Sunlight Induced Polymerization. *Eur. Polym. J.* **2021**, *147*, 110331. [CrossRef]
142. Tehfe, M.-A.; Dumur, F.; Graff, B.; Morlet-Savary, F.; Gigmes, D.; Fouassier, J.-P.; Lalevée, J. Push–Pull (Thio)Barbituric Acid Derivatives in Dye Photosensitized Radical and Cationic Polymerization Reactions under 457/473 Nm Laser Beams or Blue LEDs. *Polym. Chem.* **2013**, *4*, 3866–3875. [CrossRef]
143. Mokbel, H.; Dumur, F.; Telitel, S.; Vidal, L.; Xiao, P.; Versace, D.-L.; Tehfe, M.-A.; Morlet-Savary, F.; Graff, B.; Fouassier, J.-P.; et al. Photoinitiating Systems of Polymerization and in Situ Incorporation of Metal Nanoparticles into Polymer Matrices upon Exposure to Visible Light: Push–Pull Malonate and Malononitrile Based Dyes. *Polym. Chem.* **2013**, *4*, 5679–5687. [CrossRef]
144. Helmy, S.; Oh, S.; Leibfarth, F.A.; Hawker, C.J.; Read de Alaniz, J. Design and Synthesis of Donor–Acceptor Stenhouse Adducts: A Visible Light Photoswitch Derived from Furfural. *J. Org. Chem.* **2014**, *79*, 11316–11329. [CrossRef] [PubMed]
145. Pigot, C.; Noirbent, G.; Brunel, D.; Dumur, F. Recent Advances on Push–Pull Organic Dyes as Visible Light Photoinitiators of Polymerization. *Eur. Polym. J.* **2020**, *133*, 109797. [CrossRef]
146. Xiao, P.; Dumur, F.; Bui, T.T.; Goubard, F.; Graff, B.; Morlet-Savary, F.; Fouassier, J.P.; Gigmes, D.; Lalevée, J. Panchromatic Photopolymerizable Cationic Films Using Indoline and Squaraine Dye Based Photoinitiating Systems. *ACS Macro Lett.* **2013**, *2*, 736–740. [CrossRef]
147. Xu, Y.; Feng, T.; Yang, T.; Wei, H.; Yang, H.; Li, G.; Zhao, M.; Liu, S.; Huang, W.; Zhao, Q. Utilizing Intramolecular Photoinduced Electron Transfer to Enhance Photothermal Tumor Treatment of Aza-BODIPY-Based Near-Infrared Nanoparticles. *ACS Appl. Mater. Interfaces* **2018**, *10*, 16299–16307. [CrossRef]
148. Skotnicka, A.; Kabatc, J. New BODIPY Dyes Based on Benzoxazole as Photosensitizers in Radical Polymerization of Acrylate Monomers. *Materials* **2022**, *15*, 662. [CrossRef]
149. Lu, P.; Chung, K.-Y.; Stafford, A.; Kiker, M.; Kafle, K.; Page, Z.A. Boron Dipyrromethene (BODIPY) in Polymer Chemistry. *Polym. Chem.* **2021**, *12*, 327–348. [CrossRef]
150. Telitel, S.; Blanchard, N.; Schweizer, S.; Morlet-Savary, F.; Graff, B.; Fouassier, J.-P.; Lalevée, J. BODIPY Derivatives and Boranil as New Photoinitiating Systems of Cationic Polymerization Exhibiting a Tunable Absorption in the 400–600 Nm Spectral Range. *Polymer* **2013**, *54*, 2071–2076. [CrossRef]
151. Telitel, S.; Lalevée, J.; Blanchard, N.; Kavalli, T.; Tehfe, M.-A.; Schweizer, S.; Morlet-Savary, F.; Graff, B.; Fouassier, J.-P. Photopolymerization of Cationic Monomers and Acrylate/Divinylether Blends under Visible Light Using Pyrromethene Dyes. *Macromolecules* **2012**, *45*, 6864–6868. [CrossRef]

152. Abdallah, M.; Hijazi, A.; Graff, B.; Fouassier, J.-P.; Rodeghiero, G.; Gualandi, A.; Dumur, F.; Cozzi, P.G.; Lalevée, J. Coumarin Derivatives as Versatile Photoinitiators for 3D Printing, Polymerization in Water and Photocomposite Synthesis. *Polym. Chem.* **2019**, *10*, 872–884. [CrossRef]
153. Abdallah, M.; Dumur, F.; Hijazi, A.; Rodeghiero, G.; Gualandi, A.; Cozzi, P.G.; Lalevée, J. Keto-Coumarin Scaffold for Photoinitiators for 3D Printing and Photocomposites. *J. Polym. Sci.* **2020**, *58*, 1115–1129. [CrossRef]
154. Abdallah, M.; Hijazi, A.; Dumur, F.; Lalevée, J. Coumarins as Powerful Photosensitizers for the Cationic Polymerization of Epoxy-Silicones under Near-UV and Visible Light and Applications for 3D Printing Technology. *Molecules* **2020**, *25*, 2063. [CrossRef] [PubMed]
155. Abdallah, M.; Hijazi, A.; Cozzi, P.G.; Gualandi, A.; Dumur, F.; Lalevée, J. Boron Compounds as Additives for the Cationic Polymerization Using Coumarin Derivatives in Epoxy Silicones. *Macromol. Chem. Phys.* **2021**, *222*, 2000404. [CrossRef]
156. Chen, Q.; Yang, Q.; Gao, P.; Chi, B.; Nie, J.; He, Y. Photopolymerization of Coumarin-Containing Reversible Photoresponsive Materials Based on Wavelength Selectivity. *Ind. Eng. Chem. Res.* **2019**, *58*, 2970–2975. [CrossRef]
157. Li, Z.; Zou, X.; Zhu, G.; Liu, X.; Liu, R. Coumarin-Based Oxime Esters: Photobleachable and Versatile Unimolecular Initiators for Acrylate and Thiol-Based Click Photopolymerization under Visible Light-Emitting Diode Light Irradiation. *ACS Appl. Mater. Interfaces* **2018**, *10*, 16113–16123. [CrossRef]
158. Rahal, M.; Mokbel, H.; Graff, B.; Toufaily, J.; Hamieh, T.; Dumur, F.; Lalevée, J. Mono vs. Difunctional Coumarin as Photoinitiators in Photocomposite Synthesis and 3D Printing. *Catalysts* **2020**, *10*, 1202. [CrossRef]
159. Rajeshirke, M.; Sreenath, M.C.; Chitrambalam, S.; Joe, I.H.; Sekar, N. Enhancement of NLO Properties in OBO Fluorophores Derived from Carbazole–Coumarin Chalcones Containing Carboxylic Acid at the N-Alykl Terminal End. *J. Phys. Chem. C* **2018**, *122*, 14313–14325. [CrossRef]
160. Rahal, M.; Graff, B.; Toufaily, J.; Hamieh, T.; Dumur, F.; Lalevée, J. Design of Keto-Coumarin Based Photoinitiator for Free Radical Photopolymerization: Towards 3D Printing and Photocomposites Applications. *Eur. Polym. J.* **2021**, *154*, 110559. [CrossRef]
161. Rahal, M.; Graff, B.; Toufaily, J.; Hamieh, T.; Noirbent, G.; Gigmes, D.; Dumur, F.; Lalevée, J. 3-Carboxylic Acid and Formyl-Derived Coumarins as Photoinitiators in Photo-Oxidation or Photo-Reduction Processes for Photopolymerization upon Visible Light: Photocomposite Synthesis and 3D Printing Applications. *Molecules* **2021**, *26*, 1753. [CrossRef]
162. Hammoud, F.; Giacoletto, N.; Noirbent, G.; Graff, B.; Hijazi, A.; Nechab, M.; Gigmes, D.; Dumur, F.; Lalevée, J. Substituent Effects on the Photoinitiation Ability of Coumarin-Based Oxime-Ester Photoinitiators for Free Radical Photopolymerization. *Mater. Chem. Front.* **2021**, *5*, 8361–8370. [CrossRef]
163. Dumur, F. Recent Advances on Coumarin-Based Photoinitiators of Polymerization. *Eur. Polym. J.* **2022**, *163*, 110962. [CrossRef]
164. Liu, Z.; Dumur, F. Recent Advances on Visible Light Coumarin-Based Oxime Esters as Initiators of Polymerization. *Eur. Polym. J.* **2022**, *177*, 111449. [CrossRef]
165. Zhu, Y.; Li, L.; Zhang, Y.; Ou, Y.; Zhang, J.; Yagci, Y.; Liu, R. Broad Wavelength Sensitive Coumarin Sulfonium Salts as Photoinitiators for Cationic, Free Radical and Hybrid Photopolymerizations. *Prog. Org. Coat.* **2023**, *174*, 107272. [CrossRef]
166. Zivic, N.; Bouzrati-Zerrelli, M.; Villotte, S.; Morlet-Savary, F.; Dietlin, C.; Dumur, F.; Gigmes, D.; Fouassier, J.P.; Lalevée, J. A Novel Naphthalimide Scaffold Based Iodonium Salt as a One-Component Photoacid/Photoinitiator for Cationic and Radical Polymerization under LED Exposure. *Polym. Chem.* **2016**, *7*, 5873–5879. [CrossRef]
167. Bonardi, A.-H.; Zahouily, S.; Dietlin, C.; Graff, B.; Morlet-Savary, F.; Ibrahim-Ouali, M.; Gigmes, D.; Hoffmann, N.; Dumur, F.; Lalevée, J. New 1,8-Naphthalimide Derivatives as Photoinitiators for Free-Radical Polymerization Upon Visible Light. *Catalysts* **2019**, *9*, 637. [CrossRef]
168. Zhang, J.; Zivic, N.; Dumur, F.; Xiao, P.; Graff, B.; Fouassier, J.P.; Gigmes, D.; Lalevée, J. Naphthalimide-Tertiary Amine Derivatives as Blue-Light-Sensitive Photoinitiators. *ChemPhotoChem* **2018**, *2*, 481–489. [CrossRef]
169. Xiao, P.; Dumur, F.; Zhang, J.; Graff, B.; Gigmes, D.; Fouassier, J.P.; Lalevée, J. Naphthalimide Derivatives: Substituent Effects on the Photoinitiating Ability in Polymerizations under Near UV, Purple, White and Blue LEDs (385, 395, 405, 455, or 470 Nm). *Macromol. Chem. Phys.* **2015**, *216*, 1782–1790. [CrossRef]
170. Xiao, P.; Dumur, F.; Zhang, J.; Graff, B.; Gigmes, D.; Fouassier, J.P.; Lalevée, J. Naphthalimide-Phthalimide Derivative Based Photoinitiating Systems for Polymerization Reactions under Blue Lights. *J. Polym. Sci. Part Polym. Chem.* **2015**, *53*, 665–674. [CrossRef]
171. Zhang, J.; Zivic, N.; Dumur, F.; Xiao, P.; Graff, B.; Gigmes, D.; Fouassier, J.P.; Lalevée, J. A Benzophenone-Naphthalimide Derivative as Versatile Photoinitiator of Polymerization under near UV and Visible Lights. *J. Polym. Sci. Part Polym. Chem.* **2015**, *53*, 445–451. [CrossRef]
172. Zhang, J.; Zivic, N.; Dumur, F.; Xiao, P.; Graff, B.; Fouassier, J.P.; Gigmes, D.; Lalevée, J. N-[2-(Dimethylamino)Ethyl]-1,8-Naphthalimide Derivatives as Photoinitiators under LEDs. *Polym. Chem.* **2018**, *9*, 994–1003. [CrossRef]
173. Zhang, J.; Dumur, F.; Xiao, P.; Graff, B.; Bardelang, D.; Gigmes, D.; Fouassier, J.P.; Lalevée, J. Structure Design of Naphthalimide Derivatives: Toward Versatile Photoinitiators for Near-UV/Visible LEDs, 3D Printing, and Water-Soluble Photoinitiating Systems. *Macromolecules* **2015**, *48*, 2054–2063. [CrossRef]
174. Zhang, J.; Zivic, N.; Dumur, F.; Xiao, P.; Graff, B.; Fouassier, J.P.; Gigmes, D.; Lalevée, J. UV-Violet-Blue LED Induced Polymerizations: Specific Photoinitiating Systems at 365, 385, 395 and 405 Nm. *Polymer* **2014**, *55*, 6641–6648. [CrossRef]
175. Xiao, P.; Dumur, F.; Graff, B.; Gigmes, D.; Fouassier, J.P.; Lalevée, J. Blue Light Sensitive Dyes for Various Photopolymerization Reactions: Naphthalimide and Naphthalic Anhydride Derivatives. *Macromolecules* **2014**, *47*, 601–608. [CrossRef]

176. Xiao, P.; Dumur, F.; Frigoli, M.; Tehfe, M.-A.; Graff, B.; Fouassier, J.P.; Gigmes, D.; Lalevée, J. Naphthalimide Based Methacrylated Photoinitiators in Radical and Cationic Photopolymerization under Visible Light. *Polym. Chem.* **2013**, *4*, 5440–5448. [CrossRef]
177. Noirbent, G.; Dumur, F. Recent Advances on Naphthalic Anhydrides and 1,8-Naphthalimide-Based Photoinitiators of Polymerization. *Eur. Polym. J.* **2020**, *132*, 109702. [CrossRef]
178. Rahal, M.; Mokbel, H.; Graff, B.; Pertici, V.; Gigmes, D.; Toufaily, J.; Hamieh, T.; Dumur, F.; Lalevée, J. Naphthalimide-Based Dyes as Photoinitiators under Visible Light Irradiation and Their Applications: Photocomposite Synthesis, 3D Printing and Polymerization in Water. *ChemPhotoChem* **2021**, *5*, 476–490. [CrossRef]
179. Rahal, M.; Graff, B.; Toufaily, J.; Hamieh, T.; Ibrahim-Ouali, M.; Dumur, F.; Lalevée, J. Naphthyl-Naphthalimides as High-Performance Visible Light Photoinitiators for 3D Printing and Photocomposites Synthesis. *Catalysts* **2021**, *11*, 1269. [CrossRef]
180. Zivic, N.; Zhang, J.; Bardelang, D.; Dumur, F.; Xiao, P.; Jet, T.; Versace, D.-L.; Dietlin, C.; Morlet-Savary, F.; Graff, B.; et al. Novel Naphthalimide–Amine Based Photoinitiators Operating under Violet and Blue LEDs and Usable for Various Polymerization Reactions and Synthesis of Hydrogels. *Polym. Chem.* **2015**, *7*, 418–429. [CrossRef]
181. Xiao, P.; Dumur, F.; Graff, B.; Morlet-Savary, F.; Gigmes, D.; Fouassier, J.P.; Lalevée, J. Design of High Performance Photoinitiators at 385–405 Nm: Search around the Naphthalene Scaffold. *Macromolecules* **2014**, *47*, 973–978. [CrossRef]
182. Xiao, P.; Dumur, F.; Zhang, J.; Graff, B.; Gigmes, D.; Fouassier, J.P.; Lalevée, J. Amino and Nitro Substituted 2-Amino-1H-Benzo[de]Isoquinoline-1,3(2H)-Diones: As Versatile Photoinitiators of Polymerization from Violet-Blue LED Absorption to a Panchromatic Behavior. *Polym. Chem.* **2015**, *6*, 1171–1179. [CrossRef]
183. Chen, H.; Pieuchot, L.; Xiao, P.; Dumur, F.; Lalevée, J. Water-Soluble/Visible-Light-Sensitive Naphthalimide Derivative-Based Photoinitiating Systems: 3D Printing of Antibacterial Hydrogels. *Polym. Chem.* **2022**, *13*, 2918–2932. [CrossRef]
184. Liu, S.; Giacoletto, N.; Graff, B.; Morlet-Savary, F.; Nechab, M.; Xiao, P.; Dumur, F.; Lalevée, J. N-Naphthalimide Ester Derivatives as Type I Photoinitiators for LED Photopolymerization. *Mater. Today Chem.* **2022**, *26*, 101137. [CrossRef]
185. Mokbel, H.; Toufaily, J.; Hamieh, T.; Dumur, F.; Campolo, D.; Gigmes, D.; Fouassier, J.P.; Ortyl, J.; Lalevée, J. Specific Cationic Photoinitiators for near UV and Visible LEDs: Iodonium versus Ferrocenium Structures. *J. Appl. Polym. Sci.* **2015**, *132*, 42759. [CrossRef]
186. Villotte, S.; Gigmes, D.; Dumur, F.; Lalevée, J. Design of Iodonium Salts for UV or Near-UV LEDs for Photoacid Generator and Polymerization Purposes. *Molecules* **2020**, *25*, 149. [CrossRef]
187. Tasdelen, M.A.; Kumbaraci, V.; Jockusch, S.; Turro, N.J.; Talinli, N.; Yagci, Y. Photoacid Generation by Stepwise Two-Photon Absorption: Photoinitiated Cationic Polymerization of Cyclohexene Oxide by Using Benzodioxinone in the Presence of Iodonium Salt. *Macromolecules* **2008**, *41*, 295–297. [CrossRef]
188. Crivello, J.V.; Lam, J.H.W. Diaryliodonium Salts. A New Class of Photoinitiators for Cationic Polymerization. *Macromolecules* **1977**, *10*, 1307–1315. [CrossRef]
189. He, Y.; Zhou, W.; Wu, F.; Li, M.; Wang, E. Photoreaction and Photopolymerization Studies on Squaraine Dyes/Iodonium Salts Combination. *J. Photochem. Photobiol. Chem.* **2004**, *162*, 463–471. [CrossRef]
190. Jun, L.I.; Miaozhen, L.I.; Huaihai, S.; Yongyuan, Y.; Erjian, W. Photopolymerization Initiated by Dimethylaminochalcone/Diphenyliodonium Salt Combination System Sensitive to Visible Light. *Chin. J. Polym. Sci.* **1993**, *11*, 163–170.
191. Zivic, N.; Kuroishi, P.K.; Dumur, F.; Gigmes, D.; Dove, A.P.; Sardon, H. Recent Advances and Challenges in the Design of Organic Photoacid and Photobase Generators for Polymerizations. *Angew. Chem. Int. Ed.* **2019**, *58*, 10410–10422. [CrossRef]
192. Petko, F.; Galek, M.; Hola, E.; Topa-Skwarczyńska, M.; Tomal, W.; Jankowska, M.; Pilch, M.; Popielarz, R.; Graff, B.; Morlet-Savary, F.; et al. Symmetric Iodonium Salts Based on Benzylidene as One-Component Photoinitiators for Applications in 3D Printing. *Chem. Mater.* **2022**, *34*, 10077–10092. [CrossRef]
193. Petko, F.; Galek, M.; Hola, E.; Popielarz, R.; Ortyl, J. One-Component Cationic Photoinitiators from Tunable Benzylidene Scaffolds for 3D Printing Applications. *Macromolecules* **2021**, *54*, 7070–7087. [CrossRef]
194. Xiao, P.; Dumur, F.; Frigoli, M.; Graff, B.; Morlet-Savary, F.; Wantz, G.; Bock, H.; Fouassier, J.P.; Gigmes, D.; Lalevée, J. Perylene Derivatives as Photoinitiators in Blue Light Sensitive Cationic or Radical Curable Films and Panchromatic Thiol-Ene Polymerizable Films. *Eur. Polym. J.* **2014**, *53*, 215–222. [CrossRef]
195. Xiao, P.; Dumur, F.; Graff, B.; Gigmes, D.; Fouassier, J.P.; Lalevée, J. Red-Light-Induced Cationic Photopolymerization: Perylene Derivatives as Efficient Photoinitiators. *Macromol. Rapid Commun.* **2013**, *34*, 1452–1458. [CrossRef]
196. Dumur, F. Recent Advances on Perylene-Based Photoinitiators of Polymerization. *Eur. Polym. J.* **2021**, *159*, 110734. [CrossRef]
197. Tehfe, M.-A.; Dumur, F.; Graff, B.; Gigmes, D.; Fouassier, J.-P.; Lalevée, J. Green-Light-Induced Cationic Ring Opening Polymerization Reactions: Perylene-3,4:9,10-Bis(Dicarboximide) as Efficient Photosensitizers. *Macromol. Chem. Phys.* **2013**, *214*, 1052–1060. [CrossRef]
198. Xiao, P.; Hong, W.; Li, Y.; Dumur, F.; Graff, B.; Fouassier, J.P.; Gigmes, D.; Lalevée, J. Green Light Sensitive Diketopyrrolopyrrole Derivatives Used in Versatile Photoinitiating Systems for Photopolymerizations. *Polym. Chem.* **2014**, *5*, 2293–2300. [CrossRef]
199. Corakci, B.; Hacioglu, S.O.; Toppare, L.; Bulut, U. Long Wavelength Photosensitizers in Photoinitiated Cationic Polymerization: The Effect of Quinoxaline Derivatives on Photopolymerization. *Polymer* **2013**, *54*, 3182–3187. [CrossRef]
200. Pyszka, I.; Skowroński, Ł.; Jędrzejewska, B. Study on New Dental Materials Containing Quinoxaline-Based Photoinitiators in Terms of Exothermicity of the Photopolymerization Process. *Int. J. Mol. Sci.* **2023**, *24*, 2752. [CrossRef]
201. Pyszka, I.; Jędrzejewska, B. Photoinitiation Abilities of Indeno- and Indoloquinoxaline Derivatives and Mechanical Properties of Dental Fillings Based on Multifunctional Acrylic Monomers and Glass Ionomer. *Polymer* **2023**, *266*, 125625. [CrossRef]

202. Arsu, N.; Aydın, M. Photoinduced Free Radical Polymerization Initiated with Quinoxalines. *Angew. Makromol. Chem.* **1999**, *270*, 1–4. [CrossRef]
203. Aydın, M.; Arsu, N. Photoinitiated Free Radical Polymerization of Methylmethacrylate by Using of Quinoxalines in the Presence of Aldehydes. *Prog. Org. Coat.* **2006**, *56*, 338–342. [CrossRef]
204. Bulut, U.; Gunbas, G.E.; Toppare, L. A Quinoxaline Derivative as a Long Wavelength Photosensitizer for Diaryliodonium Salts. *J. Polym. Sci. Part Polym. Chem.* **2010**, *48*, 209–213. [CrossRef]
205. Bulut, U.; Kolay, M.; Tarkuc, S.; Udum, Y.A.; Toppare, L. Quinoxaline Derivatives as Long Wavelength Photosensitizers in Photoinitiated Cationic Polymerization of Diaryliodonium Salts. *Prog. Org. Coat.* **2012**, *73*, 215–218. [CrossRef]
206. Cao, X.; Jin, F.; Li, Y.-F.; Chen, W.-Q.; Duan, X.-M.; Yang, L.-M. Triphenylamine-Modified Quinoxaline Derivatives as Two-Photon Photoinitiators. *N. J. Chem.* **2009**, *33*, 1578–1582. [CrossRef]
207. Karaca Balta, D.; Keskin, S.; Karasu, F.; Arsu, N. Quinoxaline Derivatives as Photoinitiators in UV-Cured Coatings. *Prog. Org. Coat.* **2007**, *60*, 207–210. [CrossRef]
208. Kucybała, Z.; Pyszka, I.; Pączkowski, J. Development of New Dyeing Photoinitiators for Free Radical Polymerization Based on the 1H-Pyrazolo[3,4-b]Quinoxaline Skeleton. Part 2. *J. Chem. Soc. Perkin Trans. 2* **2000**, *7*, 1559–1567. [CrossRef]
209. Podsiadły, R.; Szymczak, A.M.; Podemska, K. The Synthesis of Novel, Visible-Wavelength, Oxidizable Polymerization Sensitizers Based on the 8-Halogeno-5,12-Dihydroquinoxalino[2,3-b]Quinoxaline Skeleton. *Dye. Pigment.* **2009**, *82*, 365–371. [CrossRef]
210. Yao, J.-Y.; Hou, H.-H.; Ma, X.-D.; Xu, H.-J.; Shi, Z.-X.; Yin, J.; Jiang, X.-S. Combining Photo-Cleavable and Hydrogen-Abstracting Groups in Quinoxaline with Thioether Bond as Hybrid Photoinitiator. *Chin. Chem. Lett.* **2017**, *28*, 6–12. [CrossRef]
211. Sun, L.; Jiang, X.; Yin, J. Study of Methoxyphenylquinoxalines (MOPQs) as Photoinitiators in the Negative Photo-Resist. *Prog. Org. Coat.* **2010**, *67*, 225–232. [CrossRef]
212. Ercan, B.T.; Gultekin, S.S.; Yesil, T.; Dincalp, H.; Koyuncu, S.; Yagci, Y.; Zafer, C. Highly Conjugated Isoindigo and Quinoxaline Dyes as Sunlight Photosensitizers for Onium Salt-Photoinitiated Cationic Polymerization of Epoxy Resins. *Polym. Int.* **2022**, *71*, 867–873. [CrossRef]
213. Tehfe, M.-A.; Lepeltier, M.; Dumur, F.; Gigmes, D.; Fouassier, J.-P.; Lalevée, J. Structural Effects in the Iridium Complex Series: Photoredox Catalysis and Photoinitiation of Polymerization Reactions under Visible Lights. *Macromol. Chem. Phys.* **2017**, *218*, 1700192. [CrossRef]
214. Dumur, F.; Bertin, D.; Gigmes, D. Iridium (III) Complexes as Promising Emitters for Solid–State Light–Emitting Electrochemical Cells (LECs). *Int. J. Nanotechnol.* **2012**, *9*, 377–395. [CrossRef]
215. Lalevée, J.; Blanchard, N.; Tehfe, M.-A.; Morlet-Savary, F.; Fouassier, J.P. Green Bulb Light Source Induced Epoxy Cationic Polymerization under Air Using Tris(2,2′-Bipyridine)Ruthenium(II) and Silyl Radicals. *Macromolecules* **2010**, *43*, 10191–10195. [CrossRef]
216. Xiao, P.; Zhang, J.; Campolo, D.; Dumur, F.; Gigmes, D.; Fouassier, J.P.; Lalevée, J. Copper and Iron Complexes as Visible-Light-Sensitive Photoinitiators of Polymerization. *J. Polym. Sci. Part Polym. Chem.* **2015**, *53*, 2673–2684. [CrossRef]
217. Garra, P.; Dumur, F.; Gigmes, D.; Al Mousawi, A.; Morlet-Savary, F.; Dietlin, C.; Fouassier, J.P.; Lalevée, J. Copper (Photo)Redox Catalyst for Radical Photopolymerization in Shadowed Areas and Access to Thick and Filled Samples. *Macromolecules* **2017**, *50*, 3761–3771. [CrossRef]
218. Mokbel, H.; Anderson, D.; Plenderleith, R.; Dietlin, C.; Morlet-Savary, F.; Dumur, F.; Gigmes, D.; Fouassier, J.-P.; Lalevée, J. Copper Photoredox Catalyst "G1": A New High Performance Photoinitiator for near-UV and Visible LEDs. *Polym. Chem.* **2017**, *8*, 5580–5592. [CrossRef]
219. Zhang, J.; Campolo, D.; Dumur, F.; Xiao, P.; Fouassier, J.P.; Gigmes, D.; Lalevée, J. Iron Complexes as Photoinitiators for Radical and Cationic Polymerization through Photoredox Catalysis Processes. *J. Polym. Sci. Part Polym. Chem.* **2015**, *53*, 42–49. [CrossRef]
220. Al Mousawi, A.; Poriel, C.; Dumur, F.; Toufaily, J.; Hamieh, T.; Fouassier, J.P.; Lalevée, J. Zinc Tetraphenylporphyrin as High Performance Visible Light Photoinitiator of Cationic Photosensitive Resins for LED Projector 3D Printing Applications. *Macromolecules* **2017**, *50*, 746–753. [CrossRef]
221. Brahmi, C.; Benltifa, M.; Vaulot, C.; Michelin, L.; Dumur, F.; Airoudj, A.; Morlet-Savary, F.; Raveau, B.; Bousselmi, L.; Lalevée, J. New Hybrid Perovskites/Polymer Composites for the Photodegradation of Organic Dyes. *Eur. Polym. J.* **2021**, *157*, 110641. [CrossRef]
222. Brahmi, C.; Benltifa, M.; Vaulot, C.; Michelin, L.; Dumur, F.; Millange, F.; Frigoli, M.; Airoudj, A.; Morlet-Savary, F.; Bousselmi, L.; et al. New Hybrid MOF/Polymer Composites for the Photodegradation of Organic Dyes. *Eur. Polym. J.* **2021**, *154*, 110560. [CrossRef]
223. Riad, K.B.; Arnold, A.A.; Claverie, J.P.; Hoa, S.V.; Wood-Adams, P.M. Photopolymerization Using Metal Oxide Semiconducting Nanoparticles for Epoxy-Based Coatings and Patterned Films. *ACS Appl. Nano Mater.* **2020**, *3*, 2875–2880. [CrossRef]
224. Shukla, S.; Pandey, P.C.; Narayan, R.J. Tunable Quantum Photoinitiators for Radical Photopolymerization. *Polymers* **2021**, *13*, 2694. [CrossRef]
225. Dumur, F. Recent Advances on Water-Soluble Photoinitiators of Polymerization. *Eur. Polym. J.* **2023**, *189*, 111942. [CrossRef]
226. Dumur, F. Recent Advances on Photobleachable Visible Light Photoinitiators of Polymerization. *Eur. Polym. J.* **2023**, *186*, 111874. [CrossRef]
227. Lalevée, J.; Fouassier, J.P. Recent Advances in Sunlight Induced Polymerization: Role of New Photoinitiating Systems Based on the Silyl Radical Chemistry. *Polym. Chem.* **2011**, *2*, 1107–1113. [CrossRef]

228. Dumur, F. Recent Advances on Photoinitiating Systems Designed for Solar Photocrosslinking Polymerization Reactions. *Eur. Polym. J.* **2023**, *189*, 111988. [CrossRef]
229. He, X.; Gao, Y.; Nie, J.; Sun, F. Methyl Benzoylformate Derivative Norrish Type I Photoinitiators for Deep-Layer Photocuring under Near-UV or Visible LED. *Macromolecules* **2021**, *54*, 3854–3864. [CrossRef]
230. Dietlin, C.; Trinh, T.T.; Schweizer, S.; Graff, B.; Morlet-Savary, F.; Noirot, P.-A.; Lalevée, J. Rational Design of Acyldiphenylphosphine Oxides as Photoinitiators of Radical Polymerization. *Macromolecules* **2019**, *52*, 7886–7893. [CrossRef]
231. Tang, Z.; Gao, Y.; Jiang, S.; Nie, J.; Sun, F. Cinnamoylformate Derivatives Photoinitiators with Excellent Photobleaching Ability and Cytocompatibility for Visible LED Photopolymerization. *Prog. Org. Coat.* **2022**, *170*, 106969. [CrossRef]
232. Bouzrati-Zerelli, M.; Kirschner, J.; Fik, C.P.; Maier, M.; Dietlin, C.; Morlet-Savary, F.; Fouassier, J.P.; Becht, J.-M.; Klee, J.E.; Lalevée, J. Silyl Glyoxylates as a New Class of High Performance Photoinitiators: Blue LED Induced Polymerization of Methacrylates in Thin and Thick Films. *Macromolecules* **2017**, *50*, 6911–6923. [CrossRef]
233. Kirschner, J.; Bouzrati-Zerelli, M.; Fouassier, J.P.; Becht, J.-M.; Klee, J.E.; Lalevée, J. Silyl Glyoxylates as High-Performance Photoinitiators for Cationic and Hybrid Polymerizations: Towards Better Polymer Mechanical Properties. *J. Polym. Sci. Part Polym. Chem.* **2019**, *57*, 1420–1429. [CrossRef]
234. Bouzrati-Zerelli, M.; Maier, M.; Fik, C.P.; Dietlin, C.; Morlet-Savary, F.; Fouassier, J.P.; Klee, J.E.; Lalevée, J. A Low Migration Phosphine to Overcome the Oxygen Inhibition in New High Performance Photoinitiating Systems for Photocurable Dental Type Resins. *Polym. Int.* **2017**, *66*, 504–511. [CrossRef]
235. Balta, D.K.; Temel, G.; Aydin, M.; Arsu, N. Thioxanthone Based Water-Soluble Photoinitiators for Acrylamide Photopolymerization. *Eur. Polym. J.* **2010**, *46*, 1374–1379. [CrossRef]
236. Corrales, T.; Catalina, F.; Allen, N.S.; Peinado, C. Novel Water Soluble Copolymers Based on Thioxanthone: Photochemistry and Photoinitiation Activity. *J. Photochem. Photobiol. Chem.* **2005**, *169*, 95–100. [CrossRef]
237. Eren, T.N.; Lalevée, J.; Avci, D. Water Soluble Polymeric Photoinitiator for Dual-Curing of Acrylates and Methacrylates. *J. Photochem. Photobiol. Chem.* **2020**, *389*, 112288. [CrossRef]
238. Eren, T.N.; Lalevée, J.; Avci, D. Bisphosphonic Acid-Functionalized Water-Soluble Photoinitiators. *Macromol. Chem. Phys.* **2019**, *220*, 1900268. [CrossRef]
239. Jiang, X.; Wang, W.; Xu, H.; Yin, J. Water-Compatible Dendritic Macrophotoinitiator Containing Thioxanthone. *J. Photochem. Photobiol. Chem.* **2006**, *181*, 233–237. [CrossRef]
240. He, X.; Jia, W.; Gao, Y.; Jiang, S.; Nie, J.; Sun, F. Water-Soluble Benzoylformic Acid Photoinitiators for Water-Based LED-Triggered Deep-Layer Photopolymerization. *Eur. Polym. J.* **2022**, *167*, 111066. [CrossRef]
241. Zeng, B.; Cai, Z.; Lalevée, J.; Yang, Q.; Lai, H.; Xiao, P.; Liu, J.; Xing, F. Cytotoxic and Cytocompatible Comparison among Seven Photoinitiators-Triggered Polymers in Different Tissue Cells. *Toxicol. In Vitro* **2021**, *72*, 105103. [CrossRef]